Seasonal Ensemble Predictions of West African Monsoon Precipitation in the ECMWF System 3 with a Focus on the AMMA Special Observing Period in 2006

ADRIAN M. TOMPKINS AND LAURA FEUDALE

Abdus Salam International Centre for Theoretical Physics, Trieste, Italy

(Manuscript received 1 December 2008, in final form 24 September 2009)

ABSTRACT

The West Africa monsoon precipitation of the ECMWF operational Seasonal Forecast System (SYS3) is evaluated at a lead time of 2–4 months in a 49-yr hindcast dataset, with special attention paid to the African Monsoon Multidisciplinary Analysis (AMMA) special observation period during 2006. In both the climatology and the year 2006 the SYS3 reproduces the progression of the West Africa monsoon but with a number of differences, most notably a southerly shift of the precipitation in the main monsoon months of July and August and the lack of preonset rainfall suppression and sudden onset jump. The model skill at predicting summer monsoon rainfall anomalies has increased in recent years indicating improvements in the ocean analysis since the 1990s.

Examination of other model fields shows a widespread warm sea surface temperature (SST) bias exceeding 1.5 K in the Gulf of Guinea throughout the monsoon months in addition to a cold bias in the North Atlantic, which would both tend to enhance rainfall over the Gulf of Guinea coast at the expense of the monsoon rainfall over the Sahel. Seasonal forecasts were repeated for 2006 using the same release of the atmospheric forecast model forced by observed SSTs, and the monsoon rainfall reverts to its observed position, indicating the importance of the SST biases.

A lack of stratocumulus off the west coast of Africa in SYS3 was hypothesized as a possible cause of the systematic rain and SST biases. Two more sets of ensembles were thus conducted with atmospheric model upgrades designed to tackle radiation, deep convection, and turbulence deficiencies. While these enhancements improve the simulation of stratocumulus significantly, it is found that the improvement in the warm SST bias is limited in scope to the southern cold tongue region. In contrast, the changes to the representation of convection cause an increase in surface downwelling shortwave radiation that, combined with latent heat flux changes associated with the wind stress field, increases the SST warm bias on and to the north of the equator. Thus, while the precipitation shortfall in the Sahel is reduced with the new physics, the overestimated rainfall of SYS3 in the coastal region is further enhanced, degrading the model systematic errors overall in the West Africa region. Finally, the difference in the systematic biases between the coupled and uncoupled systems was noted to be an impediment to the development of seamless forecasting systems.

1. Introduction

In the tropics the sea surface temperature (SST) and its spatial gradients have a significant influence on both local and remote precipitation, documented in both observational studies (Graham and Barnett 1987; Zhang 1993) and idealized integrations using cloud-resolving models (e.g., Grabowski et al. 2000; Tompkins 2001). The thermal inertia and assumed predictability of the SSTs imply that reliable seasonal predictions in the tropics are a realizable aim. This paper assesses a state-of-the-art seasonal prediction system in the region of West Africa, the subject of a recent long-term observation campaign known as the African Monsoon Multidisciplinary Analysis (AMMA), which peaked in 2006 with a high-intensity special observing period (SOP) (Janicot and Sultan 2007).

Focusing on the West Africa monsoon system, a number of studies have revealed a strong correlation with local SST in the Atlantic, Indian, and eastern Pacific Oceans (Palmer 1986; Rowell et al. 1992; Fontaine and Bigot 1993; Opokuankomah and Cordery 1994; Fontaine and Janicot 1996; Zheng et al. 1999; Vizy and Cook 2001; Giannini et al. 2003). Nevertheless, actual seasonal forecasts using dynamical models have not

Corresponding author address: Adrian M. Tompkins, Abdus Salam International Centre for Theoretical Physics, Strada Costiera 11, 34014 Trieste, Italy.
E-mail: tompkins@ictp.ita

DOI: 10.1175/2009WAF2222236.1

historically performed reliably in these regions relative to other parts of the globe (Wang et al. 2008).

This shortfall in realized model skill is due to a number of reasons. First, in terms of SSTs, global coupled models have their greatest success in the prediction of the El Niño–Southern Oscillation (ENSO) phenomenon and the associated SST anomalies in the eastern Pacific, but the influence of these anomalies is less significant in West Africa than in many other tropical regions (Ropelewski and Halpert 1987; Paeth and Friederichs 2004). Second, another oceanic region that is important for West African rainfall, especially in the coastal countries, is the tropical Atlantic. Because of the strong three-way interaction between SST anomalies, surface winds, and convection in this region (e.g., Dommenget and Latif 2000), coupled models tend to do poorly at predicting these SSTs, with many models exhibiting strong positive temperature biases. Third, while the basic monsoon dynamics in West Africa is reasonably well understood, the intraseasonal and interannual variabilities of the monsoon rains in West Africa depend on a rich array of locally interacting processes, involving deep convection, soil moisture and vegetation properties (Taylor et al. 1997; Eltahir 1998), extratropical intrusions (Roca et al. 2005), cloud and aerosol radiative forcing (Tompkins et al. 2005a), the African and tropical easterly jets (Cook 1999; Thorncroft et al. 2003), and mesoscale organized phenomena such as squall lines and African easterly waves (Albignat and Reed 1980; Diongue et al. 2002; Grist 2002; Fink and Reiner 2003; Mekonnen et al. 2006). Representing these interactions poses a particularly demanding challenge for dynamical forecast models of non-cloud-resolving resolutions. All of the above reasons can limit the skill of models in reproducing the climate and variability of the West African monsoon system.

Each year since 1998, representatives from national and international organizations in West Africa join together at the African Centre of Meteorological Application for Development (ACMAD) to consider the available statistical and dynamical seasonal forecasts and to jointly issue a probabilistic consensus forecast known as the Prévisions Saisonnières en l'Afrique de l'Ouest (PRE-SAO). The dynamical models that contribute to this process include those issued from the Met Office, Météo-France, the International Research Institute for Climate and Society (IRI), the National Centers for Environmental Prediction (NCEP), and the European Centre for Medium-Range Weather Forecasts (ECMWF). While some attempts have been and continue to be made to directly validate the consensus forecast itself (e.g., Hamatan et al. 2004), the limited sample size (11 yr) and tercile probabilistic nature of these forecasts hinder this process and imply that validation efforts remain focused on the individual contributing forecasting systems.

The ECMWF forecast model is central to the PRESAO process, but while the operational analyses and atmosphere-only medium-range forecasts have been periodically subjected to evaluation over Africa (e.g., Reed et al. 1988; Kamga et al. 2000; Tompkins et al. 2005b), this is less the case for the coupled seasonal forecast system. An earlier release of the coupled model (called system 2) has been evaluated within the context of its contribution to the Development of a European Multimodel Ensemble System for Seasonal-to-Interannual Prediction (DEMETER) forecasting system (Palmer et al. 2004), and Stockdale et al. (2006) revealed that performance in SST predictions in the tropical and southern subtropical Atlantic in this system did not exceed that of persistence, while skill in the North Atlantic and ENSO regions was demonstrated. Despite shortcomings in SST prediction in some regions, the DEMETER forecasts of precipitation were found useful for predicting malaria incidence in Botswana at 3-month lead times (Thomson et al. 2006). It should be pointed out that ENSO is generally accepted to have a greater impact on southern African rainfall than in the AMMA region of West Africa (Ropelewski and Halpert 1987; Nicholson and Selato 2000). An evaluation of the current (as of 2009) system 3 coupled system version is currently limited to the study of Molteni et al. (2007), which in addition to other regions, also examines the precipitation seasonal forecasts over West Africa, which appear to indicate skill in the Sahel region in recent years.

This paper therefore aims to supplement these earlier studies with a more systematic investigation of the system 3 operational seasonal forecast of ECMWF, concentrating on the precipitation and its systematic biases over West Africa. The modeling system is briefly introduced in the following section. As the focus is West Africa, the analysis presented here restricts itself to the main summer monsoon period. The validation uses a set of 49 hindcast ensembles conducted at ECMWF for the years 1960–2008, with additional attention paid to 2006, the year of the AMMA SOP.

2. Model and data

The Seasonal Forecast System that is evaluated here is closely related to the other ECMWF forecast systems of a single deterministic atmosphere-only l0-day forecast run twice each day and an ensemble forecast at lower resolution, which extends to 1 month using a coupled ocean model (Vitart et al. 2008). The atmospheric model component of these latter systems is usually updated several times per year, each identified with a code XXRY,

where Y is the release (R) of each code cycle XX. Some of these atmospheric model upgrades are not relevant for the seasonal forecasting system, monitoring or incorporating new observations into the analysis system, implementing new analysis system improvements, or operational technical changes. Nevertheless, a number of these upgrades incorporate major changes to the model physics parameterizations, which are mostly evaluated and developed within the uncoupled atmosphere-only framework.

In contrast, the coupled Seasonal Forecast System is updated far less frequently, partly due to the numerical expense of evaluating new systems with the large catalog of hindcast integrations required. As of 2009, the operational seasonal forecast model is currently using the third release of the coupled system, known as system 3 (hereafter SYS3). Only a brief summary of the coupled system is provided since details are presented elsewhere (see Anderson et al. 2008, and references therein). The atmospheric model is based on version number 31R1. This cycle was operational in the medium-range and ensemble systems during 2006, and was also used for the interim reanalysis. The resolution is T_L 159 with 62 vertical sigma levels. The atmosphere is coupled to the Hamburg Ocean Primitive Equation (HOPE) ocean model running with 29 vertical levels (Wolff et al. 1997).

As well as focusing on the AMMA SOP 2006, analysis of hindcast integrations is presented, which were made at ECMWF with four start dates per year for the years from 1960 to the present for the European Union's (EU) ENSEMBLES project. The main interest is the West African monsoon period, which occurs during July–September (JAS); therefore, the analysis is restricted to the 1 May forecasts, implying a 2–4-month lead time for the monsoon. This start date is also pertinent, since it is the 1 May integrations that contribute to the PRESAO consensus forecast process.

Each forecast consists of 11 ensemble member integrations. The ensemble members are initialized with perturbed SSTs created by introducing surface wind anomalies in the ocean analysis system that represent the wind uncertainty. Vialard et al. (2005) compared this perturbation method to other alternatives and noted that all methods led to a lack of spread in the 2–4-month range, pointing to multimodel ensembles as the solution.

The data used for validation purposes is summarized in Table 1. As the paper concentrates on precipitation forecast biases, three different datasets are used for this parameter. Monthly station data of the Climatic Research Unit (CRU; Mitchell and Jones 2005) provide the longest continuous time series for validation in the presatellite era. The Global Precipitation Climatology Project (GPCP) merges station data with satellite information and thus suffers less from sampling biases in regions with sporadic data availability. The Famine Early Warning System (FEWS) daily estimates are also a merged product of the Geostationary Operational Environmental Satellite (GOES) precipitation index (GPI), Special Sensor Microwave Imager (SSM/I), and Advanced Microwave Sounding Unit (AMSU) platforms combined with those surface gauge measurements reported on the global telecommunications system. Daily data have greater uncertainty, but they are used to provide information concerning the subseasonal temporal variations.

TABLE 1. Datasets used for validation.

Parameter	Data	Resolution	Reference
SST	OISST	1.0°	Reynolds et al. (2002)
Cloud cover	ISCCP	2.5°	Rossow and Schiffer (1991)
Radiative flux	CERES	2.5°	Wielicki et al. (1996)
10-m winds	QuikSCAT	25 km	Hoffman and Leidner (2005)
10-m winds	SSM/I	1.0°	Wentz (1997)
Precipitation	CRU	0.5°	Mitchell and Jones (2005)
Precipitation	GPCP	2.5°	Huffman et al. (1995)
Precipitation	FEWS	0.1°	Herman et al. (1997)

For statistical significance estimates when comparing model mean fields, very simple fixed error estimates are used of 0.05 for the International Satellite Cloud Climatology Project (ISCCP) total cloud cover (Rossow et al. 1993) and 15% of rainfall for version 2 (v2) of the GPCP data (Adler et al. 2003). For monthly mean fields the uncertainty of scatterometer winds is estimated as 0.7 m s^{-1} (H. Hersbach, ECMWF, 2008, personal communication). Error estimates for Clouds and the Earth's Radiant Energy System (CERES) monthly radiative budgets at the top of the atmosphere were given as 2.5 W m^{-1} for shortwave and 1.9 W m^{-1} for longwave radiation by Wielicki et al. (1995).

3. Hindcast rainfall assessment

The mean JAS precipitation is compared with CRU station data in Fig. 1 for 1960–2002 and to GPCP for a shorter period (1979–2007). This comparison reveals that the model is able to reproduce the distribution of rainfall reasonably well with the peak over the West African coast in addition to the orographically forced local maxima over the Cameroonian and Ethiopian Highlands. There are obvious shortcomings in the monsoon precipitation climatology, with an underestimation over eastern Africa (although station data are sparse in

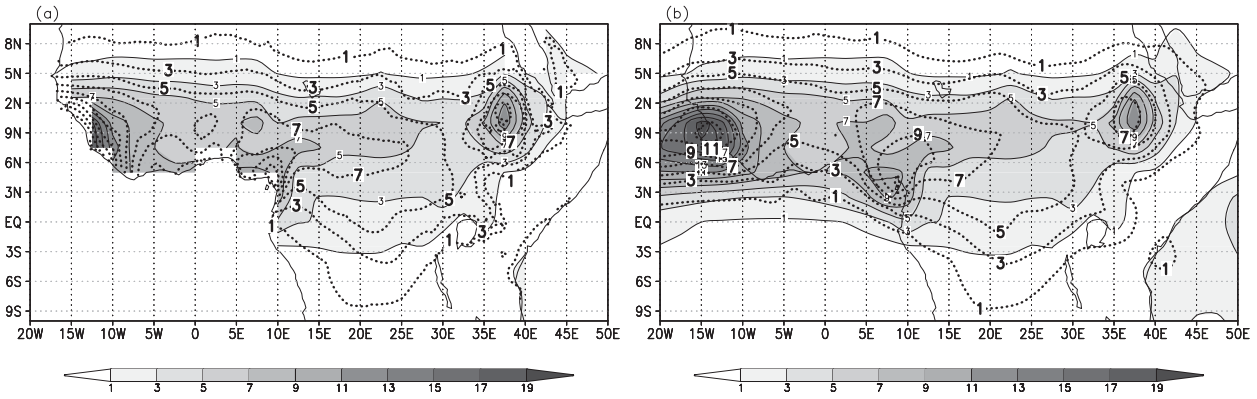

FIG. 1. JAS mean anomaly precipitation of the SYS3 ensemble mean (shaded) compared with observations dataset displayed with a dotted contour line. SYS3 compared with (a) CRU for the 1960–2002 time period and (b) GPCP for the 1979–2007 time period. With the exception of a thin belt of points along the coast of Nigeria, all differences were found to be significant at the 95% level. Units are mm day^{-1}.

some regions there, especially for recent periods). It is apparent that the rain in the West African monsoon is displaced too far south in the model.

The onset of the rainfall is examined in a Hovmöller diagram, comparing the model to GPCP in order to be able to include the rainfall over the Gulf of Guinea (Fig. 2). The comparison shows again the southerly displacement of the rainfall. Another shortcoming of the mean seasonal rainfall distribution regards the preonset period of rainfall suppression, documented by Sultan and Janicot (2003), during which the precipitation over the coastal regions is reduced, while the ''jump'' of the rainband that marks the onset is yet to occur. The cause of this shortcoming requires a complete and accepted theory describing the African monsoon's onset. Ramel et al. (2006) and Hagos and Cook (2007) have, respectively, highlighted the shift in the position of the Saharan heat low and described the rainfall jump in terms of inertial instability. Moreover, Sultan and Janicot (2003) propose that the temporary suppression of deep convection in both the Sahel and also at the Guinea coast during the transition phase could result from increased advection of midtroposphere dry air as the heat low intensifies. Entrainment of midtropospheric dry air can suppress deep convection, although the situation is complicated in the region of the African easterly jet, since the low-level shear is conducive for squall lines, which can be enhanced by dry midtropospheres, and indeed Roca et al. (2005) produce evidence for dry-air intrusions increasing convective activity at certain times of the year. The suppression of the convection would be temporary, lasting until the enhanced monsoon humidity flux allows deep convection onset in the Sahel (Sultan et al. 2007). The reproduction of this effect in models would rely on them representing the vertical humidity structure and its impacts on convection well, which, as Derbyshire et al. (2004) demonstrated, is a task that many current state-of-the-art models fail to accomplish.

Figure 3 shows the latitudinal variation of the rainfall during the preonset and monsoon main phases, averaging the rainfall for the model and the observations of GPCP and CRU averaged over a longitude of 10°W–10°E and for the period of 1979–2007. The latitude variation of the model rainfall agrees very well with all observations during the onset month of June, and likewise during the recession month of September. However, the peak months of July and August reveal the systematic biases apparent in the rainfall maps, namely an underestimation northward of 10°N, and a significant overestimation to the south. In general, the difference between the model ensemble mean and the observations mean exceeds both the intra-ensemble spread and the disparity between the observational datasets, although it should be stated that the datasets are not independent, as station data are used in GPCP products. The model rainfall between 14° and 16°N is only half that of the observations.

The year-to-year prediction of the seasonal rainfall anomaly for the Sahel region from 10° to 20°N and 10°W to 10°E (Fig. 4a) reveals apparent limited ability to predict JAS rainfall from the 1 May start date, with positive anomalies predicted in many of the drought years, including 1983 and 1984. It is notable that in the latter years the model is able to reproduce an upward trend in rainfall that was also observed, while the general change from wet to drought conditions from the 1960s to the 1980s was not reproduced. If the anomaly around a 10-yr running mean average is examined, the model predicts the correct sign of the rainfall anomaly in all but 1 of the last 10 yr

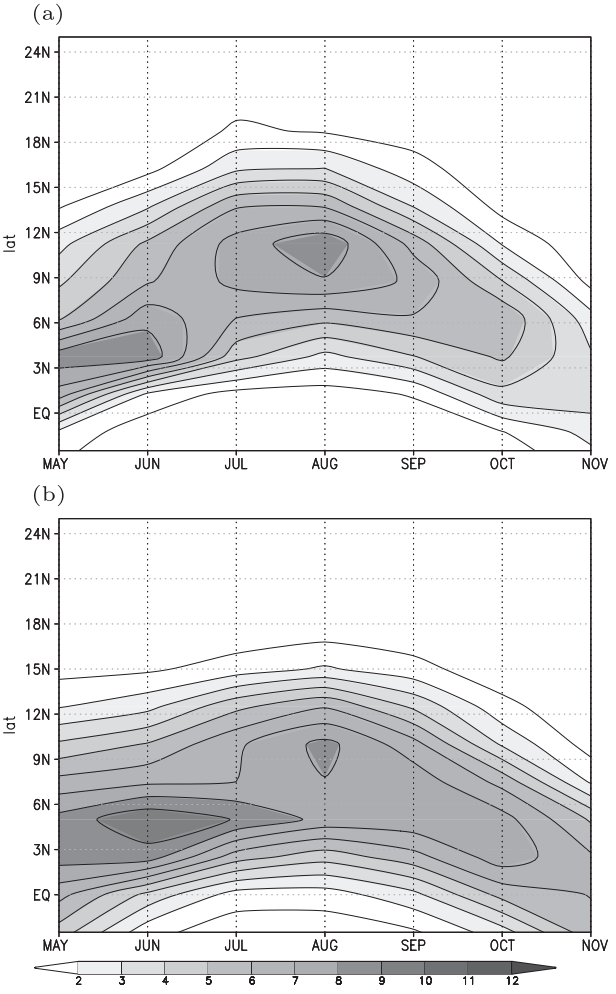

FIG. 2. The 1979–2007 zonal (10°W–10°E) average Hovmöller plot of rainfall from (a) GPCP observations and (b) the model ensemble mean (mm day^{-1}).

(not shown), agreeing with the findings of Molteni et al. (2007). However, the magnitude of the ensemble average rainfall anomaly is underpredicted.

Deterministic seasonal hindcast skill is assessed using the metric recommended by the World Meteorological Organization, which provides the percentage improvement in the mean square error over a climatological hindcast. This is referred to as the mean square skill score (MSSS), defined as (e.g., Murphy and Epstein 1989)

$$\mathrm{MSSS} = 1 - \frac{\mathrm{MSE}_f}{\mathrm{MSE}_{\mathrm{cl}}} \tag{1}$$

$$= 1 - \frac{\frac{1}{n}\sum_{i=1}^{n}(\hat{x}_i - x_i)^2}{\frac{1}{n}\sum_{i=1}^{n}x_i^2}, \tag{2}$$

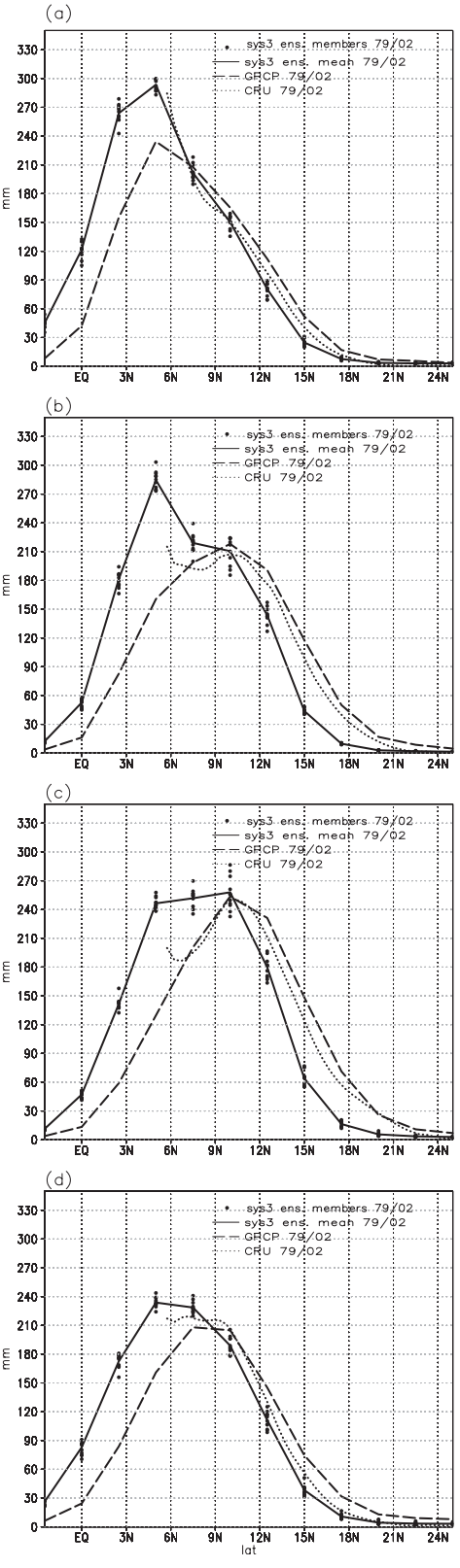

FIG. 3. The 10°W–10°E ensemble mean rainfall averages compared to CRU and GPCP over the period 1979–2002 for (a) June, (b) July, (c) August, and (d) September.

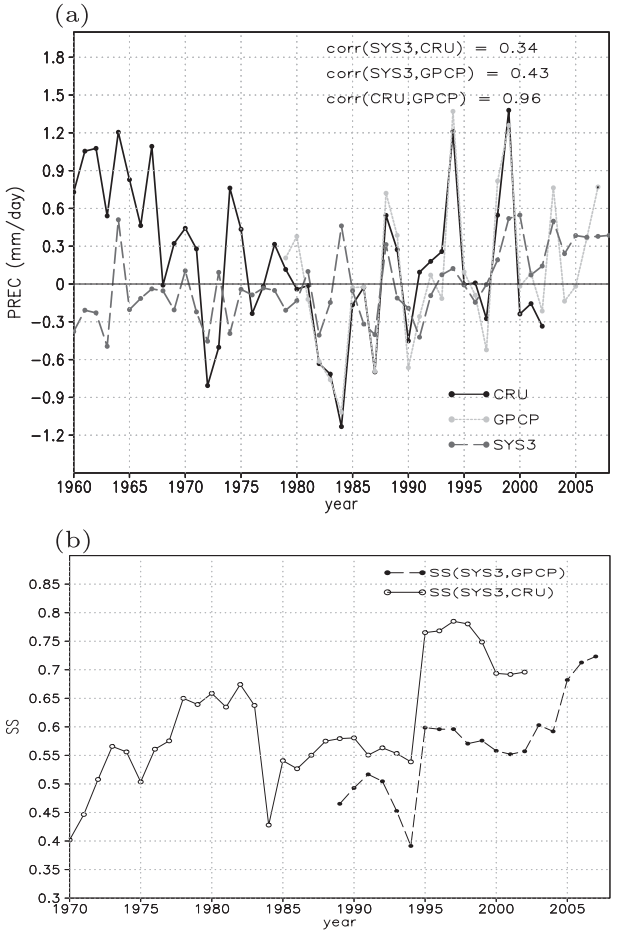

FIG. 4. Time series of 10°–20°N, 10°W–10°E box average JAS precipitation: (a) anomaly (mm day^{-1}), with respect to the 20-yr (1981–2000) mean period comparing CRU (black, 1960–2000) and GPCP (light gray, 1979–2007) to SYS3 (dark gray, 1960–2008). The correlation is calculated for the 1981–2000 period, and (b) MSSS, removing the prior 10 yr to eradicate decadal trends.

where MSE_f and $\mathrm{MSE}_{\mathrm{cl}}$ are, respectively, the mean squared error of the hindcasts and the mean squared error of the climatology hindcasts. Here, $\hat{x}_i$ and x_i are, respectively, the hindcast and observed anomaly values for each of the n years. A 10-yr running average of MSSS for the Sahel mean JAS rainfall shows a general upward trend, although the dip in skill associated with the poor forecasts for the drought years of the early 1980s is apparent (Fig. 4b).

The fact that both the prediction of the decadal trend and the interannual variability improves from the mid-1990s, reflected in increased skill scores, indicates that the quality of the ocean observing system (and the resulting ocean analysis) was not sufficient during the earlier decades since the forecast modeling system is identical for all periods. Indeed, it was only in the late 1990s that the Pilot Research Moored Array in the Tropical Atlantic (PIRATA) array was first installed in the Atlantic (Servain et al. 1998). Measurements such as these were shown to be important for the analysis and forecasts by Vidard et al. (2007), and the extension of the Tropical Atmosphere Ocean (TAO) array into the Indian Ocean was also a recent new source of data.

The skill of any model precipitation estimate is obviously affected by the averaging area, and the skill in the Sahel-averaged precipitation is not reflected when assessing the model on a point-wise basis. A spatial map of the 2.5° resolution point-wise JAS rainfall anomaly correlation at a 2–4-month lead time of SYS3 against GPCP observations for the period 1979–2007 reveals correlations of less than 0.2 for most of Africa (not shown). There is a Sahel band of low but positive correlation (0.2–0.4, not statistically significant), which appears to be derived from the ability of the model to reproduce the recent upward long-term rainfall trend, since subtracting an 11-yr running average from both the model and observations before performing the anomaly correlation (following Giannini et al. 2003) also reduces the point-wise skill to near zero in the Sahel.

The systematic bias of the rainfall climatology is likely to detrimentally impact the skill of the model. Given adequate observations, systematic climate biases can be addressed with local point-wise bias correction methodologies such as the cumulative distribution function based correction technique (Hopson 2006; Ines and Hansen 2006; Piani et al. 2009) or techniques such as the singular value decomposition method applied in Kang et al. (2004). Here, we apply a very simple correction by progressively shifting the target area to determine which latitudinal offset maximizes the correlation between the observations and the model forecasts. The impacts on the rainfall correlation of the systematic southerly shift of the rainband are assessed and the correlation (and forecast skill) is found to be maximized when the model rainfall is shifted 3° or 4° in latitude to the north, depending on the validation dataset used (Fig. 5).

4. Focus on AMMA SOP 2006

a. Subseasonal variability

The subseasonal temporal variability of rainfall is important component for models to simulate correctly, especially if the model forecasts are used to drive application models for crop and water resources (e.g., Challinor et al. 2003; Hopson 2006). Reproducing the correct variability of rainfall in this region is challenging for models, as convective cells are often highly organized in systems such as squall lines and are embedded in and interact with African easterly waves (Duvel 1990;

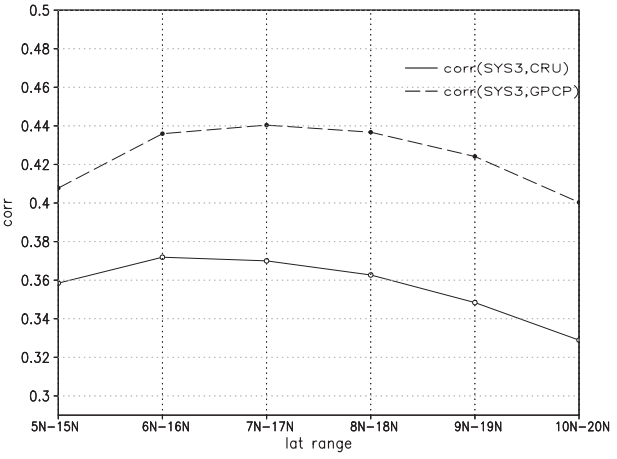

FIG. 5. Mean JAS correlation between observed rainfall (CRU, 1960–2002; GPCP, 1979–2007) in the region 10°–20°N and 10°W–10°E, and the model rainfall averaged between 10°W and 10°E and over the latitude range given along the horizontal axis.

Diedhiou et al. 1999; Fink and Reiner 2003; Berry and Thorncroft 2005; Lavaysse et al. 2006). The variability of the rainfall in the model and observations is examined using the wavelet analysis technique that reveals how the dominant modes of variability change in time (Torrence and Compo 1998). The analysis is conducted on a time series of the mean rainfall for the region 10°–20°N and 10°W–10°E. The analysis of the daily FEWS data for 2006 shows intermittent power during the months of July and August (Fig. 6b). During these months there are two distinct peaks in power at around 3–9 days and around 15 days, agreeing with the findings of Janicot and Sultan (2001) and Sultan et al. (2003), using a similar analysis technique. FEWS data from other years between 2000 and 2007 show similar features (not shown). The higher-frequency variability is directly associated with the passage of African easterly waves (AEWs) (Diedhiou et al. 1999; Sultan et al. 2003), while the 15-day modulation is distinct from AEW activity, which Mounier et al. (2008) recently claimed is linked to a feedback between convectively generated cloud, surface short radiative fluxes, and the surface pressure gradients. The analysis in Fig. 6 discards variability exceeding 32 days and thus does not include the modulation associated with the MJO as demonstrated by Janicot and Sultan (2001, their Fig. 1), Matthews (2004), and Maloney et al. (2008).

Analyzing one example integration in the forecast ensemble, the model in comparison has no clear peak associated with AEW activity, and with the exception of two events has relatively little power at time scales less than 5 days. Instead, the model rainfall is modulated more at the longer post-10-day time scales. The incorrect representation of short-term variability in the model implies that statistical corrections for subseasonal variability may also be required if the model is to be used to drive end-user models such as regional crop models, as the total seasonal yield in rainfall-limited (non irrigated) regions depends strongly on the variability of the rainfall and not just the mean amount (Challinor et al. 2003).

To focus on the AMMA SOP onset, Fig. 7 shows a time–latitude plot of rainfall for the 1 May 2006 forecast, compared to daily rainfall data from FEWS. In both cases a running mean with a window of 5 days is used to smooth some of the day-to-day fluctuations. Figure 7 shows the general progression northward of the rainfall associated with the onset of the monsoon, and the relative southerly shift of the rainband in the model is clear.

In 2006, the onset was severely delayed relative to the climatological average, which is around 24 June with a standard deviation of approximately 1 week (Fontaine et al. 2008). The delayed onset has been partly attributed to the passage of a Madden–Julian oscillation (MJO) event by Janicot and Sultan (2007) and Janicot et al. (2008). Drobinski et al. (2009) discuss the role of the interaction between the African easterly jet, AEWs, and the Harmattan winds, while Marin et al. (2009) highlight

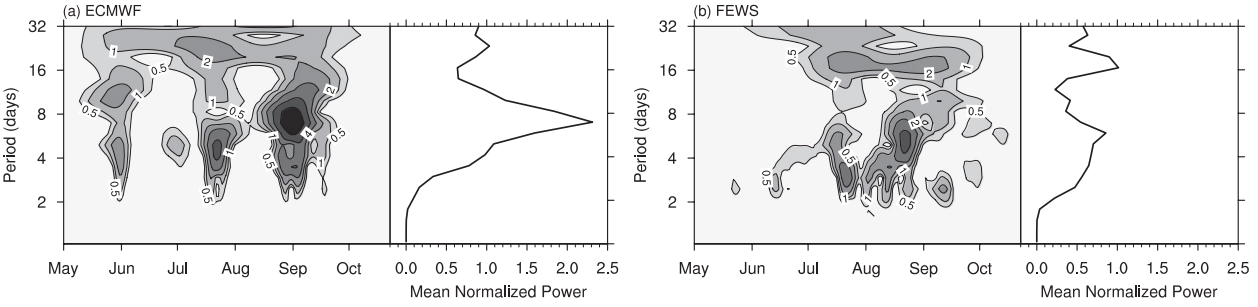

FIG. 6. Wavelet analysis of the time series of rainfall from 1 May 2006 for the region 10°–20°N and 10°W–10°E for (a) SYS3 forecast control ensemble member 0 and (b) the FEWS rainfall dataset. (left sides) The temporal evolution of the normalized wavelet power (as in Fig. 1 of Janicot and Sultan 2001). (right sides) The averages of the wavelet power across the whole forecast time.

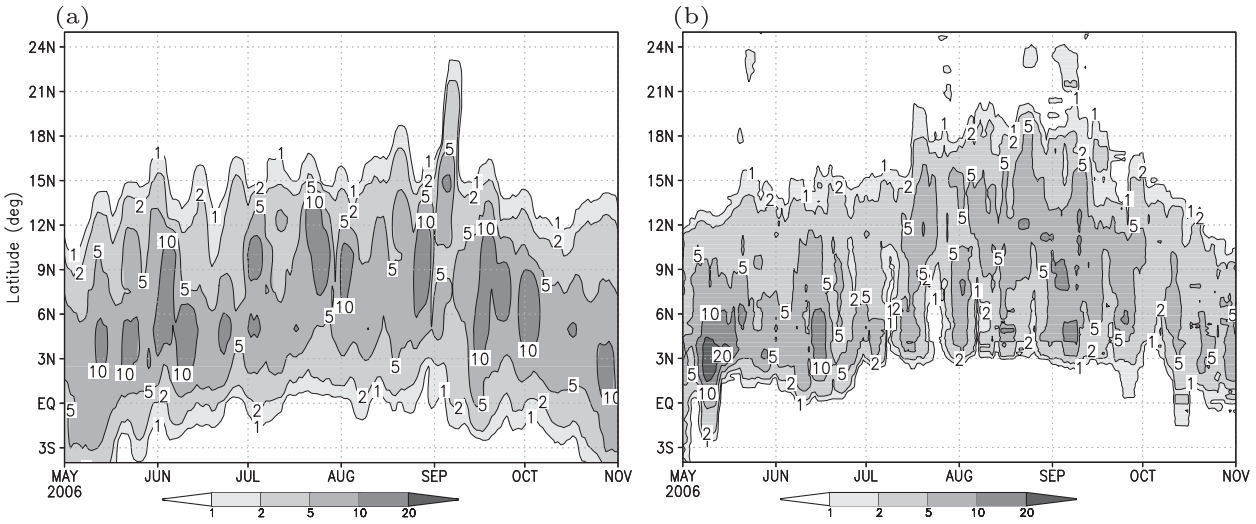

FIG. 7. Hovmöller diagram of rainfall averages between 10°W and 10°E for (a) SYS3 ensemble member 0 and (b) FEWS with a 5-day running mean applied (mm day^{-1}).

the fact that the Atlantic equatorial cold tongue development was delayed in 2006 producing a significant SST warm anomaly. The FEWS observations show that the northerly extent of the rain undergoes a rapid transition around 10 July, and the peak rainfalls shift to between 10° and 15°N after this point. In contrast, while the model does forecast a shift in the peak rainfall during July and August, with maxima occurring around 10°N, there is no evidence of any shift in the northern boundary of significant rainfall, which remains fixed at 15°N from mid-May to September, with the exception of an intriguing event that reaches as far 20°N in both the model and the observations at the start of September. In addition to this forecast, this event is predicted by 2 other ensemble members from the ensemble of 11 (not shown).

b. Seasonal mean statistics

Comparing the 2006 JAS rainfall from SYS3 to GPCP retrievals shows that the systematic bias of the southerly shift is also clearly visible in the AMMA SOP year (Fig. 8a). The monthly evolution of the rainfall difference map reveals that the problem is present in each individual month. The biases in July and August reflect the seasonal mean pattern. In September the southerly shift is notable where the model rains too much over the Gulf of Guinea, while precipitation is underestimated almost throughout West Africa, although it will be noted later that GPCP products could overestimate the precipitation over the Sahel during the monsoon. Figures 8e–h show the JAS rainfall biases for other years between 2002 and 2005 and show how robust the error signal is from year to year.

The top-of-the-atmosphere (TOA) infrared flux is often used as a proxy for convective activity. The difference map (Fig. 9) shows a large region over West Africa where the biases are negative (TOA IR flux is assigned positive downward), signifying too high outgoing longwave radiation. This agrees with the previous precipitation biases, indicating a lack of deep convection in the Sahel in this model cycle, although it should be recalled that TOA infrared flux information is used in the GPCP rainfall retrieval algorithms. The model biases in IR could result from a lack of upper-level cloud cover, not enough cloud ice, or deep convective clouds detraining at an altitude that is too low.

Past examination of model-simulated Meteosat 11-μm channel brightness temperature animations by the first author using the methodology of Morcrette (1989) and Chevallier and Kelly (2002) indicates part of the error is due to the lack of high cirrus cloud that is advected northward, cloud that would not produce surface precipitation. This raises the possibility that GPCP rainfall products, which use IR information in their retrievals, may in fact overestimate rainfall in the northern reaches of the Sahel affected by the advected cirrus cloud. Indeed, referring back to Fig. 3, it is seen that GPCP rainfall amounts exceed the CRU station data northward of 10°N in each month from June to September.

5. Discussion

Convection responds to a host of interacting dynamic and thermodynamic forcings, which can impact the vertical thermodynamic profile and the associated convective available potential energy (CAPE) and convective

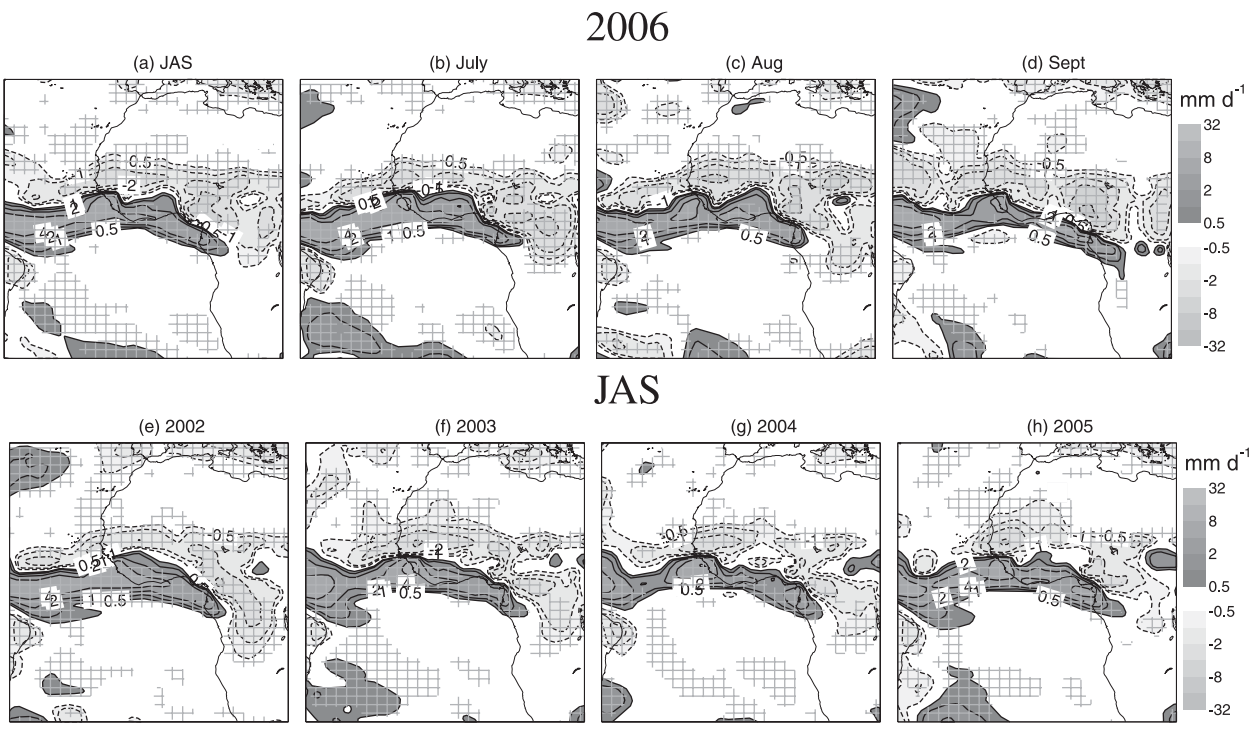

FIG. 8. SYS3 ensemble mean precipitation bias relative to GPCP v2 for (a) JAS, (b) July, (c) August, and (d) September 2006, and (e) JAS 2002, (f) JAS 2003, (g) JAS 2004, and (h) JAS 2005. The hatched area indicates regions where the difference is significant at the 95% level, and negative contours are shown with dashed lines.

inhibition (Parker 2002). Thus, the convective suppression may occur via atmospheric stabilization by radiative heating or importation of dry air into the Sahel at low levels, such as would be the case if the heat low were too deep in the model simulation. Tompkins et al. (2005a) found that an earlier atmospheric model version suffered from the convection migrating too far north during the forecast. Changes to the specified aerosol climatology in the region that reduced the aerosol optical depth over the Sahara and the Sahel had a strong impact on convection activity primarily through the shortwave (SW) radiation budget. The influence was twofold, with a reduction in atmospheric SW heating through aerosol absorption leading to an increase in radiative stabilization of the free troposphere. At the same time, the increase in the surface incoming solar radiation drives a deeper and more vigorous dry convective boundary layer over the heat low region. The reaction in the medium-range forecast included the prevention of the northward propagation of deep convection and strengthened the forecasted African easterly jet.

Other reasons for the rainfall remaining too far south could be associated with factors that alter the low-level moist static energy budget, in which Thorncroft et al. (2003) documented biases in the model analyses using an older-model cycle operational in the year 2000. A too dry boundary layer could result from a dry land surface [shown to be potentially important in Douville and Chauvin (2000)], and replacing the land surface scheme with a soil moisture history derived using observed precipitation has a small but nevertheless positive impact on rainfall in the Sahel, moving the rainband slightly

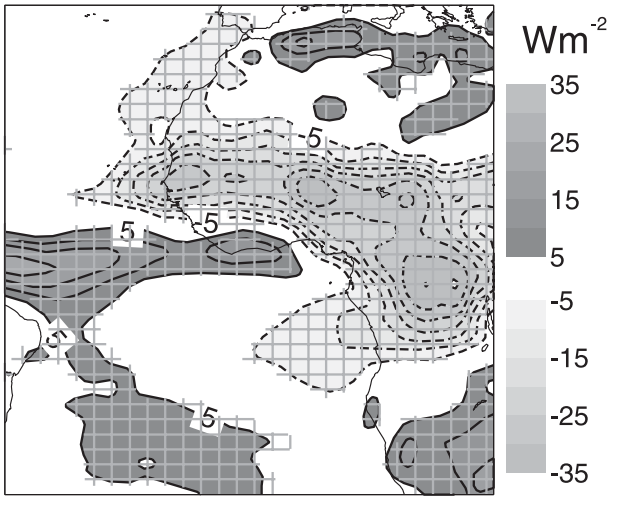

FIG. 9. TOA IR bias (model–CERES) for JAS 2006. The hatched area indicates regions where the difference is significant at the 95% level.

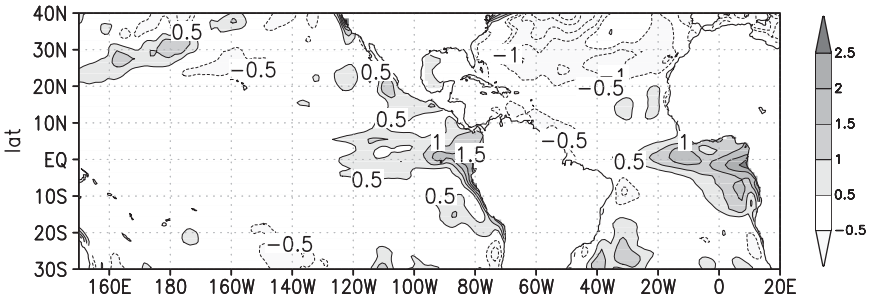

FIG. 10. JAS 2006 SST bias of the SYS3 forecasts compared to OISST dataset (K).

northward in the model simulations (A. Agusti-Panareda et al. 2009). The humidity and pressure gradients are also affected by the Saharan heat low; thus, representations of both the land surface properties over the Sahara and dry convective processes are also likely to be important. A weakened monsoon flow, possibly by too much shear-driven mixing of the nocturnal jet (Parker et al. 2005), may also play a role. To conclude, it is evident that deficiencies in the dry, shallow, and deep convective schemes may be involved.

A further factor concerns the SSTs in the Gulf of Guinea. Warm SST anomalies in the Gulf of Guinea increase the boundary layer moist static energy of the low-level monsoon flow, but primarily favor local deep convection over the gulf, suppressing activity to the north. Warmer SSTs in the gulf have been partly blamed for the extended decadal dry spell in the Sahel, for example, along with a general warming in the Indian Ocean (Giannini et al. 2003; Held et al. 2005). On intraseasonal time scales, the impacts of the cold tongue's development on enhancing the northward progression of the monsoon rain were shown in sensitivity tests by Okumura and Xie (2004), while the late development of the cold SSTs in the Gulf of Guinea was also suggested to play a role in the late onset of the monsoon in 2006 (Janicot et al. 2008). By extension, models suffering from warm SST biases in the Gulf of Guinea will tend to exhibit increased convection over the gulf and along the Guinean coast at the expense of Sahelian rainfall. The mean seasonal forecast SST evolution over the monsoon period (Fig. 10) reveals the development of a strong positive bias over the tropical and southern Atlantic, which exceeds 2 K at its peak. The SST bias in the northern Atlantic Ocean is negative, on the other hand, which would also contribute to an increase in the north–south gradient of SST and further prevent northern migration of monsoon rainfall (Palmer 1986). The SYS3 biases in the tropical Atlantic are seen to far exceed those anywhere in the Pacific basin, including the El Niño forecasting regions in the central and eastern Pacific, which form the benchmark for seasonal forecast system assessment. The warm ocean bias coincides with the development of the cold tongue in the eastern Atlantic (Mitchell and Wallace 1992). The bias could be associated with the ocean model's representation of the mixed layer considering its 10-m vertical resolution there, with Blanke and Delecluse (1993) highlighting the influence of the turbulent mixing formulation on SST in the region. The warm bias is not restricted to the location of the cold tongue waters however, since there is also a significant warm bias in the Northern Hemisphere between the equator and the Guinea coastline at 5°N.

Recent research efforts have identified variations in surface wind-driven latent heat flux anomalies as the major factor in driving tropical Atlantic SST variability (Dommenget and Latif 2000; Frankignoul and Kestenare 2005; Yu et al. 2006). Thus, the root cause of the SST bias does not have to lie with the ocean model HOPE. The atmosphere–ocean system in this region is tightly coupled, with ocean surface temperature anomalies driven by low-level wind biases but in turn affecting the distribution and strength of the convection and the associated low-level atmospheric dynamics. The positive feedback of such a two-way coupling between the ocean and atmosphere can amplify the effects of incorrectly represented atmospheric physics.

One such shortcoming in the atmospheric model is apparent from the errors in the shortwave (SW) TOA fluxes (Fig. 11a). A bias exceeding a 30 W m^{-2} peak and 10 W m^{-2} over a wide area occurs off the west coast of the continent at 15°S in the regions typically covered with stratocumulus cloud and subject to coastal upwelling. Underestimation of stratocumulus cloud cover and liquid water path is a common global model problem (e.g., Hannay et al. 2009), and the increase in downward SW radiation at the surface would lead to a significant SST warm anomaly. A radiative bias of 30 W m^{-2} distributed over a mixed layer depth of 50 m results in a bias exceeding 1.5 K after a month for example, on the order of the typical model biases.

The errors in the SW budget are confirmed by the model biases in total cloud cover (Fig. 11b), revealing

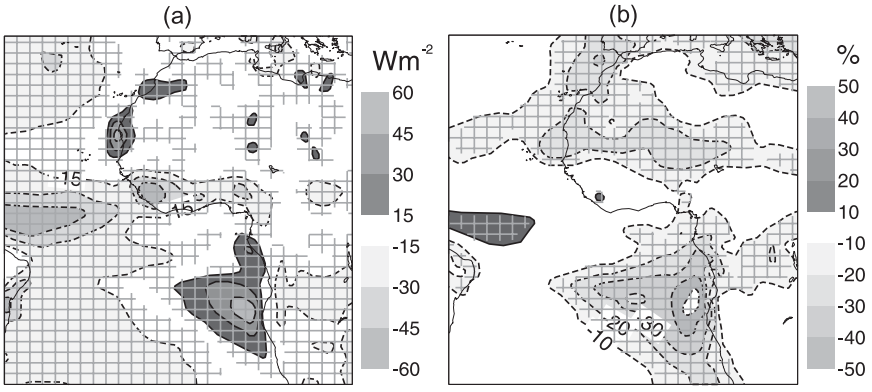

FIG. 11. For JAS 2006, (a) TOA SW radiative flux bias and (b) total cloud cover bias in absolute percent. The hatched area indicates regions where the difference is significant at the 95% level.

a significant negative bias in cloud cover in the stratocumulus regions. There is also an underestimate of the total column liquid water path in the same regions, exceeding 50 g m^{-2}, compared to version 6 retrievals from SSM/I (Wentz 1997) (not shown). The surface SW budget is harder to determine from observations over the oceans; however, as the predominant cloud type in this region in JAS is shallow stratocumulus, the TOA biases are likely to reflect those at the surface. The surface downwelling radiation in the region exceeds the (climatology) estimates of da Silva et al. (1994) by more than 40 W m^{-2} across the region, for example (not shown).

Winds biases are an important factor for determining surface latent and sensible heat fluxes, and Huang et al. (2004) indicate that wind stress is the major determinant of the SST variability in the southern tropical Atlantic (STA) mode. Under representing local wind speeds leads to inadequate convective precipitation in atmosphere-only uncoupled models (Miller et al. 1992). In a coupled model, this is complicated by the fact that surface flux anomalies cannot alter the local moist static energy budget integrated across the planetary boundary layer and the ocean surface mixed layer. Thus, although the SST will warm in response to low local wind conditions, while the low wind speeds persist, such SST anomalies cannot sustain enhanced deep convection. In the coupled system, surface winds also determine the depth of the thermocline and the evolution of the cold equatorial tongue, with low wind speed anomalies along the equator leading to warm anomalies in the Gulf of Guinea (e.g., Verstraete 1992). Wind stress in the southern Atlantic is also important, and Marin et al. (2009) recently contrasted the cold tongue evolutions in 2005 and 2006, showing how the reduced surface wind stress in the southern Atlantic in 2006 led to late cold tongue development.

A positive wind bias off the west coast of Africa is seen in Fig. 12. This bias extends across the tropical Atlantic south of the equator, although this is smaller than the assumed rms error of the QuikSCAT instrument retrievals and intra-ensemble spread, implying that the systematic biases are not significant there. Moreover, this southern Atlantic bias is not apparent when winds are validated using SSM/I retrievals (not shown). In contrast, north of the equator both satellite retrievals indicate that the model suffers from low wind speeds, with the QuikSCAT bias vector showing the model has a northerly bias. The monsoon flow is thus weakened in the model, and the patterns of the wind biases are consistent with the rainfall biases discussed earlier, with too much convection predicted over the Atlantic leading to the strong convergence zone pattern there. The low

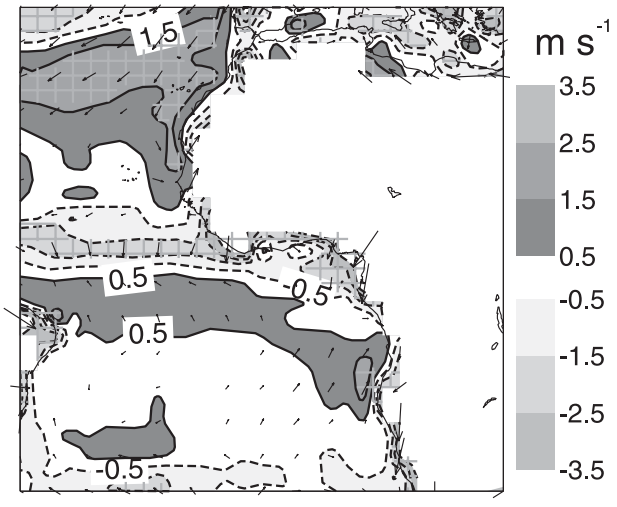

FIG. 12. JAS 2006 SYS3 bias for 10-m winds compared to QuikSCAT.

wind speeds across the Atlantic north of the equator would lead to reduced surface latent heat fluxes and enhanced SSTs.

In summary, it appears that deficiencies in the model physics that lead to the underrepresentation of stratocumulus cloud and too low surface winds north of the equator could contribute to the warm SST biases observed during JAS 2006. Assuming very simply that SST biases are locally controlled, then it is possible that the warm bias in the Gulf of Guinea has two distinct origins, with the SW radiative flux errors dominating in the cold tongue region to the south of the equator and wind errors being more important north of the equator. Richter and Xie (2008) cite examples of Coupled Model Intercomparison Project (CMIP) coupled climate models where this is also the case.

6. Sensitivity tests

To investigate the root of some the SYS3 systematic biases in further detail and the potential to tackle these in the near future in the coupled system, three further sets of 9- or 11-member ensemble integrations were performed, as outlined in Table 2. The first experiment (SST31R1) isolates the effects of the global SST biases by repeating the integrations using the identical atmospheric model cycle (31R1), but in uncoupled mode by imposing observed SSTs [version 2 of the optimal interpolation SST dataset (OISSTv2); Reynolds et al. (2002)]. A second set of experiments then investigates the impacts of upgraded model physics on the West African systematic biases by rerunning the uncoupled experiment using model cycle 35R2 (SST35R2). This model cycle was used operationally in 2009 for the medium-range high-resolution deterministic forecast and the recently combined ensemble and monthly forecasts, described in Vitart et al. (2008). Thus, the upgrades to the physical parameterizations represent all the operational changes to these latter systems between 2006 and 2009, and are the changes that will need to be included in the seasonal forecast model of ECMWF to revert to a seamless system with uniform model physics across all forecast time scales.

Changes to the model included the implementation of the Rapid Radiative Transfer Model (RRTM) shortwave radiation scheme (Mlawer and Clough 1997) with the Monte Carlo Independent Column Approximation (McICA) treatment of cloud overlap (Pincus et al. 2003; Barker et al. 2008); modifications to the subgrid-scale mixing scheme, which were important for stratocumulus representation (Köhler 2005); and significant alterations to the parameterization of deep convection, altering the convective mass-flux scheme closure time scale and the treatment of convective entrainment, rendering convection more sensitive to water vapor without suppressing the convection parameterization activity. Many of these upgrades are described in Bechtold et al. (2008) and Jung et al. (2009, manuscript submitted to *Quart. J. Roy. Meteor. Soc.*) documenting improvements in the simulation of tropical convection and its variability. Specifically, the revised model

- increases the convective activity over land;
- improves the global distribution of the convective activity, including the Walker cell, and the tropical Atlantic;
- improves the midlatitude synoptic activity and the tropical variability such as Kelvin waves and the Madden–Julian oscillation and the forecasting of AEWs in one case study presented; and
- improves the representation of stratocumulus cloud.

After making the step of examining these physics upgrades in uncoupled mode, the final integration (HOPE35R2) couples the upgraded atmospheric model to the HOPE ocean model. Computing resources restricted the uncoupled integrations to a short set of years from 2002 to 2006. However, the above analysis indicates that many of the documented biases are systematic and appear in the hindcast climate as well as in the AMMA SOP year integrations.

TABLE 2. Model experiments conducted in addition to the control integration of SYS3 for the years 2002–06 with May starts and *N* ensemble members.

Expt	N	Cycle	Ocean
SYS3 (control)	11	31R1	Coupled HOPE
SST31R1	11	31R1	Uncoupled observed SSTs
SST35R2	11	35R2	Uncoupled observed SSTs
HOPE35R2	9	35R2	Coupled HOPE

a. Effect of coupling

When the precipitation errors relative to the GPCP data are compared in Fig. 13, the significant impacts of the SST are obvious. The dipole bias seen in Fig. 8a is absent in the forecast ensemble using the imposed observed SSTs (Fig. 13a), and rainfall moves farther north into the Sahel region, confirming the impacts that the SST biases in the coupled model have on restraining the northward migration of the modeled monsoon.

It is interesting to note that these results appear to conflict with earlier work with the uncoupled operational model used in 10-day forecasts, which was documented to have a too southerly shift of precipitation and a lack of convection over the Sahel. Tompkins et al. (2007) noted an underprediction of convection generally

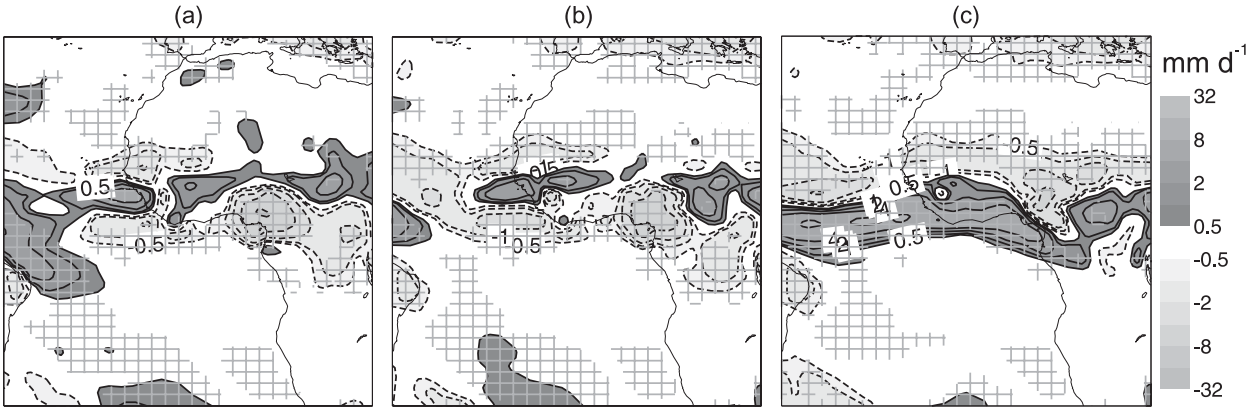

FIG. 13. As in Fig. 8a, but for (a) SST31R1, (b) SST35R2, and (c) HOPE35R2.

over the tropical continents including Africa in the uncoupled model cycle 31R1, for example. However, these biases only affect the model in the short range (less than 5 days), and already by day 10 the forecasted rainfall has shifted northward substantially. This indicates that although the southerly systematic shift of rainfall appears similar in the seasonal forecast and the short-range uncoupled forecasts, the origin is very distinct, with the former caused by coupled ocean–atmosphere feedbacks and the latter derived from an imbalance between the forecast model and its model analyses that provide the forecast initial conditions.

b. Upgraded 2009 model physics: Uncoupled

The uncoupled integrations using the improved model physics show similar patterns of rainfall biases for 2006 over Africa (Fig. 13b). The changes in the physics increased the parameterized convective rainfall over the African continent during JAS 2006 at the expense of the convective activity over the Atlantic (Fig. 14a). However, most of the increase over West Africa was balanced by an equivalent reduction in large-scale rainfall due to the suppression of grid-scale convective events (Fig. 14b). The net change over Africa in total precipitation was a small improvement, with increases over the western Sahel and a reduction over the Guinea coast, but these changes were small relative to the model biases (Fig. 14c). Thus, the total convective heating over the Sahel region is constrained by the radiative heating rate and the low-level moisture supply. The patterns in these rainfall changes are reflected systematically in each of the other years of the ensemble integrations from 2002 to 2005 and are not a feature of the 2006 circulation (not shown).

One marked improvement with the revised model physics is the simulation of the stratocumulus regime off the coast of Angola (Fig. 15a). Cloud cover increases, exceeding 30%, and the associated greater liquid water paths reduce the downward shortwave radiation at the surface by more than 30 W m^{-2} (Fig. 15b). It is also notable that even though the net precipitation over Sahel is not altered significantly, the diverse treatment of the microphysics in the convective scheme and the large-scale stratiform scheme (Tiedtke 1993) (which would operate in grid-scale convection) leads to a 10% (absolute) increase in the medium and high cloud cover over the Sahel with an associated increase in the cloud ice water path. However, there is a large decrease in the liquid water path in the area, which dominates the shortwave radiation budget and increases the downwelling SW radiation at the surface there (Fig. 15b), which is balanced by a matching increase in surface (mostly sensible) heat fluxes.

c. Upgraded 2009 model physics: Coupled

The effects of the modified physics are now examined in a coupled mode, by comparing HOPE35R2 with the SYS3 control integrations, to determine if the improvements seen in the atmosphere-only model are retained when the ocean is permitted to respond. The analysis is divided into two periods, namely the preonset months of May and June, and the monsoon season of JAS.

As expected from the uncoupled integrations, the upgraded model physics also impact the rainfall significantly in the fully coupled model, with total rainfall also decreasing in the central Atlantic in the preonset period (Fig. 16). There is an increase in the convection over the African continent, extending into the Gulf of Guinea. Associated with the precipitation and cloud changes are significant alterations to the surface radiative fluxes, with increased downwelling SW in the central Atlantic, and also over the northern Gulf of

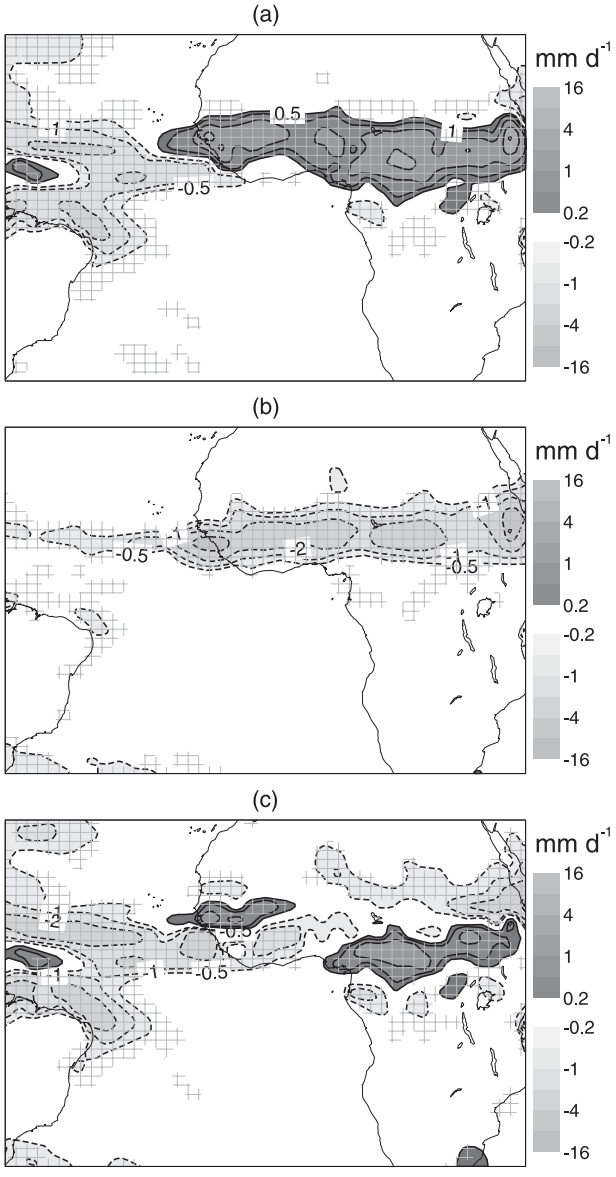

FIG. 14. Ensemble mean SST35R2 − SST31R1 differences for JAS 2006 for (a) convective precipitation, (b) large-scale precipitation, and (c) total precipitation [(a) + (b)]. The hatched area indicates regions where the difference is significant at the 95% level.

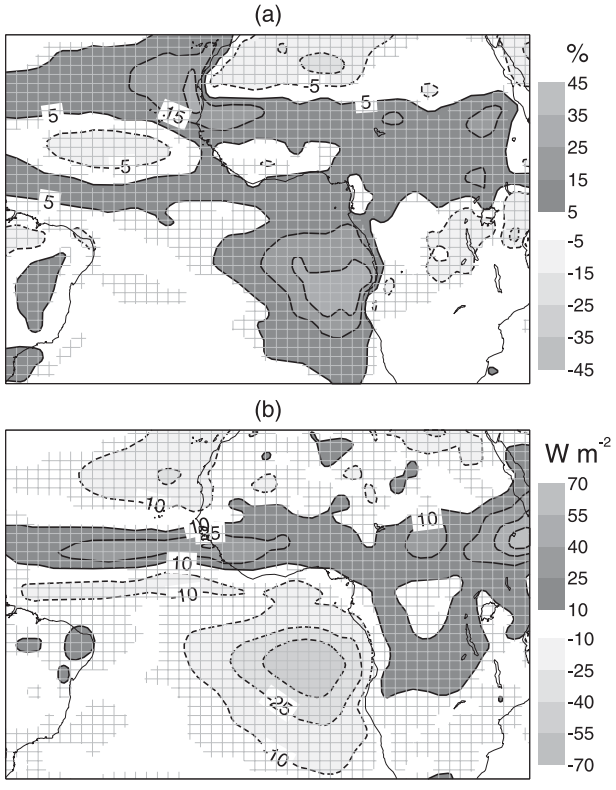

FIG. 15. Ensemble mean SST35R2 − SST31R1 differences for JAS 2006 for (a) total cloud cover and (b) surface solar radiation. Statistically significant differences are marked with hatched shading.

Guinea for the microphysical reasons given earlier. In contrast, an increase in cloudiness in the stratocumulus regions reduces the downwelling shortwave radiation. The net surface budget in the stratocumulus regions though is not greatly altered, since the decrease in SW due to stratocumulus is partly offset by their impact on the surface infrared budget. On and near the equator, the latent heat flux also contributes to the net surface heat budget changes, due to wind stress alterations. The convective increase over the eastern Gulf of Guinea between 20°W and 10°E reduces the meridional wind stress and associated surface fluxes, contributing to a warming tendency of the ocean on and north of the equator. These convective increases and the associated reduction over the central tropical Atlantic west of 20°W also impact the zonal wind stress and act to deepen the thermocline and mixed layer depth in the east while reducing it in the west.

The result of the net flux changes at the surface on the SST tendency during the first 2 months of the forecast is not beneficial for the model biases across the equatorial Atlantic, since the coupled model with the updated physics is over 0.5 K warmer in this region that already suffers from warm biases compared to the observations in SYS3 (Fig. 17a).

In the main monsoon season, the convection moves inland over the Sahel, and then HOPE35R2 has increased positive meridional wind stress associated with increased southerlies (Fig. 18), which act in tandem with the decreased SW surface downwelling radiation to give an increased net cooling tendency exceeding 25 W m^{-2} throughout the equatorial Atlantic and cold tongue region. Interestingly, the increased SST warm bias that has

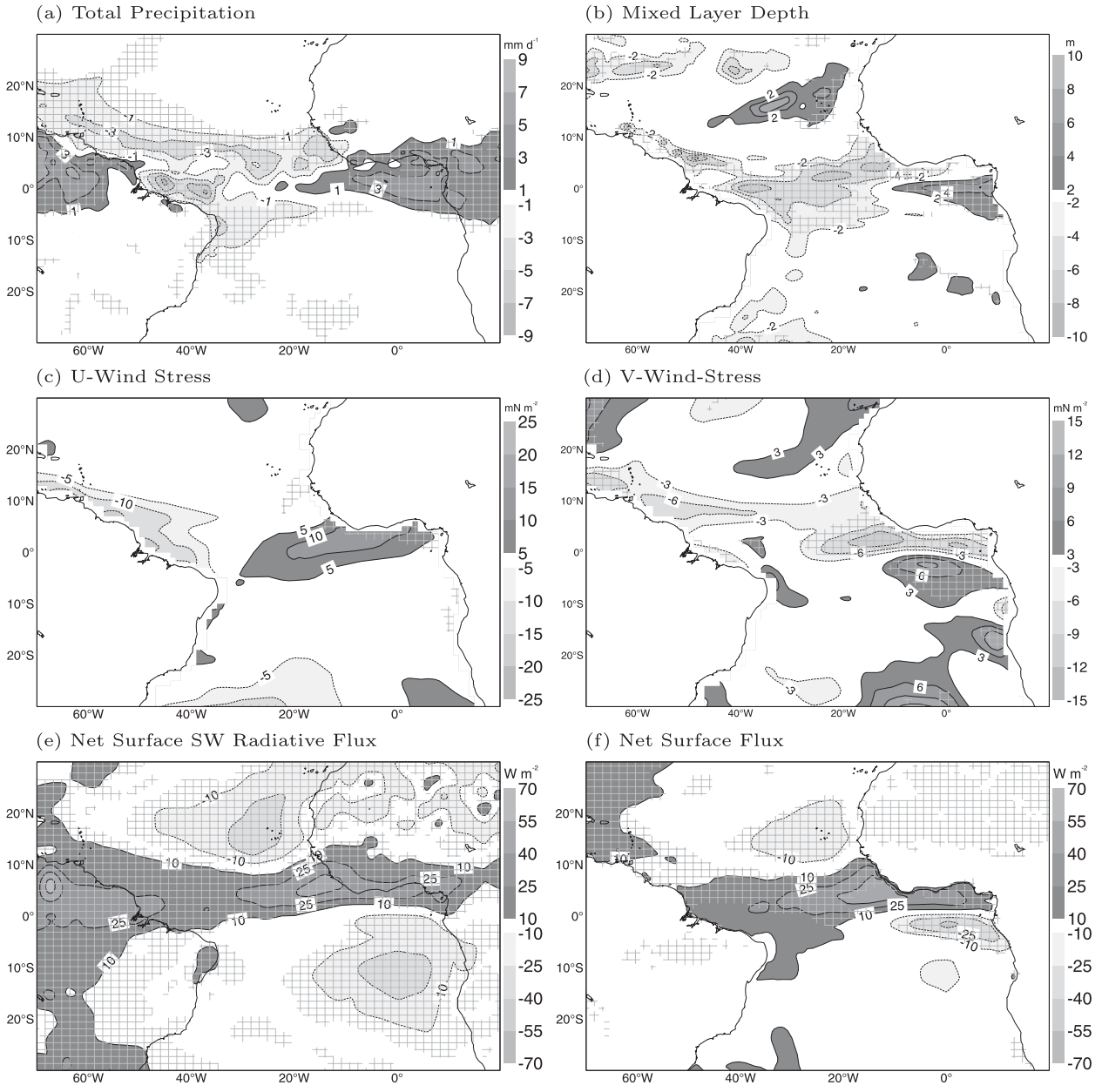

FIG. 16. Differences between HOPE35R2 and SYS3 for the months of May–June 2006 during the preonset in (a) precipitation, (b) mixed layer depth, (c),(d) *U*/*V* wind stress components, (e) net surface SW radiative flux, and (f) net surface flux, where positive numbers are the net heat gained by the surface. Statistically significant differences are marked with hatched shading.

been established by 1 July appears able to sustain an increase in the net precipitation over the continent that was not the case when SSTs were imposed in SST35R2. Thus, although the coupled model shows an increase in the total precipitation in the western Sahel (between 10° and 15°N), mimicking the uncoupled model, this is not compensated by a reduction along the Guinea coast. Instead, the precipitation is increased along the coast, which degrades the model since coastal rainfall during the JAS monsoon was already overestimated in SYS3.

The 35R2 physics leads to a relative cooling of the tropical and southern Atlantic during this period (Fig. 17b). The net effects in terms of HOPE35R2 SST biases are shown in Fig. 17c. Referring back to Fig. 10 for the SYS3 biases, it is seen that the Atlantic warm bias for JAS 2006 is increased in the new model between the equator and the gulf coast, while the bias is improved to

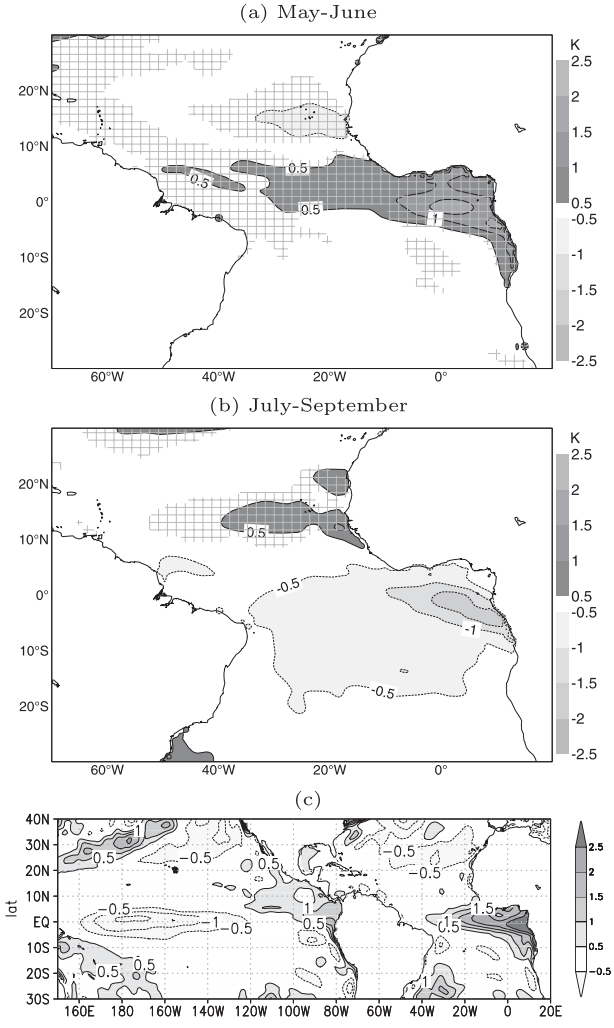

FIG. 17. HOPE35R2 − SYS3 difference in the absolute SST tendency (K) over the (a) preonset period of May/June 2006 and (b) JAS 2006, where statistically significant differences are marked with hatched shading, and (c) JAS 2006 mean SST bias (K) of the HOPE35R2 ensemble-mean seasonal forecast.

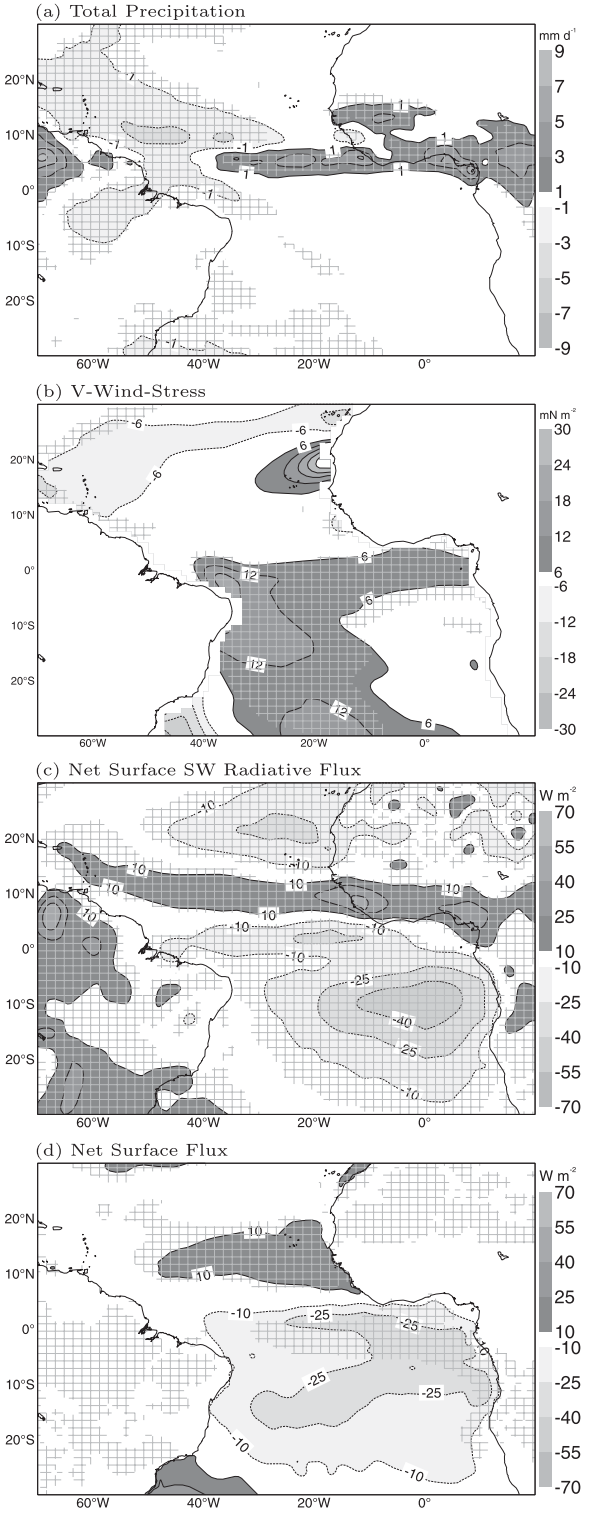

FIG. 18. Differences between HOPE35R2 and SYS3 for JAS 2006 in (a) precipitation, (b) *V* wind stress component, (c) net surface SW radiative flux, and (d) net surface flux (IR and SW radiation and latent and sensible heat flux), where positive numbers are the net heat gained by the surface. Statistically significant differences are highlighted with hatched shading.

the south of the equator in the cold tongue region. The northern Atlantic still suffers from a cold bias although its magnitude is reduced.

To summarize, it appears that the physics changes that lead to an increase in stratocumulus, while altering the surface SW radiation budget, had a limited impact on the model systematic biases in precipitation and circulation. Instead, it appears that the changes to the convection scheme had a greater impact, in particular the increase in convective activity and the associated changes to the SW radiative budget in the tropics. This is not to say that changes to other model components could not have contributed to the impacts on the radiative budgets, not least the updates to the radiative scheme itself, but a definitive assessment of each model

component is not possible without conducting a further series of experiments with each change tested in isolation, which is beyond the scope of the present article.

7. Conclusions

The ECMWF SYS3 operational seasonal forecast model integrations that are initialized each 1 May are an important component of the yearly PRE-SAO consensus seasonal forecast conducted for the West African monsoon region. It is therefore important to validate this system within the context of its representation of the African monsoon system, with this article focusing on forecasts of precipitation. The investigation examined a 49-yr set of seasonal hindcasts using 11 ensemble members to examine climatological biases, while additionally documenting some of the specific details of 2006, the AMMA SOP year.

Using CRU, GPCP, and FEWS rainfall data, the model was found to reproduce the monsoon progression into the Sahel during July–September, but with a number of differences to the observations. The main difference was the fact that the model rainfall was displaced to the south, with too much precipitation over the north coast of the Gulf of Guinea during the main monsoon season, and an underprediction north of 12°N. These biases were evident both in the long-term model summer climate in the region and specifically in 2006. Concerning the onset and intraseasonal variability, the model did not reproduce the characteristics of the monsoon onset ''jump'' and did not show any signs of the period of rainfall depression prior to onset either in general or in 2006 in particular. The northern boundary of the smaller rainfall amounts did not undergo any displacement during the onset and remained fixed at approximately 15°N throughout most of JJA. The skill of predicting the seasonal mean rainfall anomaly in JAS has improved over time in tandem with improvements in the quality of the ocean analysis as Atlantic Ocean monitoring increases.

Examining the temporal variability of the daily rainfall, the observations showed a clear spectral peak associated with intermittent African easterly wave activity and a separate peak at 15 days, both of which have been documented previously. The model was unable to reproduce these spectral features with no clear separation of the rainfall variability associated with AEWs. This was true for 2006 and all years from 2001 onward for which FEWS data are available.

The model forecasts were then compared to a number of other datasets to confirm and attempt to explain the possible origins of some of the rainfall biases, in particular the southerly shift in the monsoon rainfall. Analysis of the top-of-the-atmosphere IR budgets confirms the rainfall biases, although it should be recalled that such datasets contribute to the satellite rainfall retrieval algorithms and thus do not represent a completely independent dataset.

One possible contributory cause of the southerly rainfall shift was a significant Atlantic SST bias that developed during the summer months. This bias would tend to enhance deep convection over the northern coasts of the Gulf of Guinea and suppress rainfall to the north, as seen in the model forecasts. To investigate this, the forecasts were repeated using an identical atmospheric model but with observed SSTs imposed. The dipole rainfall bias signal was absent in this experiment, with deep convection reaching much farther into the continent.

The surface flux budgets revealed that the downwelling SW radiation at the surface was too high in the model off the west coast of Angola because of a lack of stratocumulus cloud, and it was hypothesized that this could be one contributory factor to the warm SST and associated rainfall biases. It should be emphasized that the operational seasonal forecast SYS3 is using the atmospheric model cycle 31R1, which was operational in the medium-range model during 2006. It is a continuous task of operational centers to attempt to introduce model physics and structure changes to tackle such biases as discussed here, and the medium-range and monthly forecast systems since 2006 have incorporated a variety of physics changes that were designed to target known model deficiencies, including the lack of stratocumulus.

A second set of ensemble integrations were therefore analyzed to assess the revised model physics of atmosphere version 35R2 in both the coupled and uncoupled modes. This cycle, operational in 2009 in the medium-range and monthly systems, includes major upgrades to the turbulence mixing scheme, the deep convection scheme, and the radiation schemes. Using observed SSTs, these changes were found to significantly improve the simulation of stratocumulus, and alter the balance between convectively parameterized and grid-cell convection. With imposed SSTs the total amount of the precipitation over the West African landmass showed little change. However, the associated cloud properties changed considerably, which had the result of allowing more SW radiation to reach the surface in deep convecting areas, while reducing it in stratocumulus regimes, although in the latter case this was partially offset by increased downwelling IR from the cloud. The southern Atlantic warm bias in the cold tongue region is improved as a result of the stratocumulus increases. In contrast, the SW increases on and to the north of the

equator in the deep convective regimes combine with lower winds and latent heat fluxes to make the warm bias significantly worse there. The result is that while the coupled model is able to increase the net precipitation over West Africa, most of the increases are concentrated along the northern coast of the Gulf of Guinea in JAS, degrading the SYS3 climate, which already overpredicted precipitation there during the monsoon season. This highlights the complexity of tackling systematic biases in global coupled models.

Two final points of note to make concern the robustness of the response and the potential to develop seamless forecasting systems. Despite the fact that interannual variability is large in this part of the world, the model biases and the impacts of the physics changes dominate and the precipitation bias maps for 2006 were similar for the other ensemble integrations from 2002 to 2005, even though the SST state in the Atlantic cold tongue region differed so much between 2005 and 2006. This implies that model developers testing model physics changes, often requiring large volumes of tuning integrations to maximize revised model skill, may presently use a numerically cheap integration framework of a single year, confident in the knowledge that the changes will translate successfully to other years. This will only remain the case while model systematic biases continue to exceed the interannual variability.

The final comment concerns the drive toward seamless forecasting, where seamless in this context refers to the use of uniform model physics across a wide range of forecasting time scales (e.g., Vitart et al. 2008). The ECMWF forecast model has been demonstrated to have a systematic southerly shift in rainfall in the coupled mode, and the short-range forecasts with imposed SSTs also suffer from a similar bias. However, this bias must have distinct origins in the two systems since integrating the model with imposed SST past two weeks shows a northward migration of the rain belt to approximately its correct location. Thus, methods that assess short-range forecasts to judge climate model integrations, such as suggested by Rodwell and Palmer (2007), may not be valid if a short-range uncoupled model is used to assess a coupled system.

The changes that were made in between the 2006 model cycle 31R1 and the more recent cycle 35R2 were selected and implemented after an exhaustive development and testing regime that showed a net gain in the medium-range forecast skill in the uncoupled system. That these changes have not yet been implemented into a revised seasonal forecasting system reflects the fact that, not withstanding the documented deterioration in some aspects of the modeled Africa climate, the coupled model also suffers from an unacceptable systematic cold bias in the critical central Pacific area (see Fig. 17c). This highlights the complexity of developing physical parameterizations that can perform well in both coupled and uncoupled models across a wide range of time scales in the so-called seamless forecast approach, especially if the performance metric by which the models are judged also changes with the time scale.

Acknowledgments. The extended set of SYS3 hindcasts, as well as the 35R2 coupled integration, were conducted by the ECMWF seasonal forecasting group as a contribution toward the EUFP6 ENSEMBLES project. The uncoupled integrations were performed using ECMWF computing facilities. The authors would especially like to thank Tim Stockdale for advice on the use of the hindcasts, and Franco Molteni for discussions on the science. Three anonymous reviewers also greatly improved the paper content.

The GPCP combined precipitation data were developed and computed by the NASA Goddard Space Flight Center's Laboratory for Atmospheres as a contribution to the GEWEX Global Precipitation Climatology Project. The originators of all datasets used in this paper are acknowledged for making their valuable resources freely and publically available. This research was supported by the Research grant *Fondo Integrativo Speciale per la Ricerca* of the *Centro Euro-Mediterraneo per i Cambiamenti Climatici* (FISR-CMCC).

REFERENCES

Adler, R. F., and Coauthors, 2003: The version-2 Global Precipitation Climatology Project (GPCP) monthly precipitation analysis (1979–present). *J. Hydrometeor.,* **4,** 1147–1167.

Agusti-Panareda, A., G. Balsamo, and A. Beljaars, 2009: Impact of improved soil moisture on the ECMWF precipitation forecasts in West Africa. ECMWF Tech. Memo. 611, 9 pp. [Available online at http://www.ecmwf.int/publications/library/ecpublications/_pdf/tm/601-700/tm611.pdf.]

Albignat, J. P., and R. J. Reed, 1980: The origin and structure of easterly waves in the lower troposphere in North Africa. *Mon. Wea. Rev.,* **108,** 1827–1839.

Anderson, D., and Coauthors, cited 2008: Development of the ECMWF Seasonal Forecast System, 3. ECMWF Tech. Rep. [Available online at http://www.ecmwf.int/publications.]

Barker, H. W., J. N. S. Cole, J. J. Morcrette, R. Pincus, P. Räisänen, K. von Salzen, and P. A. Vaillancourt, 2008: The Monte Carlo independent column approximation: An assessment using several global atmospheric models. *Quart. J. Roy. Meteor. Soc.,* **134,** 1463–1478.

Bechtold, P., M. Kohler, T. Jung, F. Doblas-Reyes, M. Leutbecher, M. J. Rodwell, F. Vitart, and G. Balsamo, 2008: Advances in simulating atmospheric variability with the ECMWF model: From synoptic to decadal time-scales. *Quart. J. Roy. Meteor. Soc.,* **134,** 1337–1352.

Berry, G. J., and C. Thorncroft, 2005: Case study of an intense African easterly wave. *Mon. Wea. Rev.,* **133,** 752–766.

Blanke, B., and P. Delecluse, 1993: Variability of the tropical Atlantic Ocean simulated by a general circulation model with two different mixed-layer physics. *J. Phys. Oceanogr.,* **23,** 1363–1388.

Challinor, A. J., J. M. Slingo, T. R. Wheeler, P. Q. Craufurd, and D. I. F. Grimes, 2003: Toward a combined seasonal weather and crop productivity forecasting system: Determination of the working spatial scale. *J. Appl. Meteor.,* **42,** 175–192.

Chevallier, F., and G. Kelly, 2002: Model clouds as seen from space: Comparison with geostationary imagery in the 11-μm window channel. *Mon. Wea. Rev.,* **130,** 712–722.

Cook, K. H., 1999: Generation of the African easterly jet and its role in determining West African precipitation. *J. Climate,* **12,** 1165–1184.

da Silva, A., C. C. Young, and S. Levitus, 1994: *Algorithms and Procedures*. Vol. 1, *Atlas of Surface Marine Data 1994,* NOAA/NESDIS Tech. Rep., 83 pp.

Derbyshire, S. H., I. Beau, P. Bechtold, J.-Y. Grandpeix, J.-M. Piriou, J.-L. Redelsperger, and P. M. M. Soares, 2004: Sensitivity of moist convection to environmental humidity. *Quart. J. Roy. Meteor. Soc.,* **130,** 3055–3079.

Diedhiou, A., S. Janicot, A. Viltard, P. de Felice, and H. Laurent, 1999: Easterly wave regimes and associated convection over West Africa and tropical Atlantic: Results from the NCEP/NCAR and ECMWF reanalyses. *Climate Dyn.,* **15,** 795–822.

Diongue, A., J.-P. Lafore, J.-L. Redelsperger, and R. Roca, 2002: Numerical study of a Sahelian synoptic weather system: Initiation and mature stages of convection and its interactions with the large-scale dynamics. *Quart. J. Roy. Meteor. Soc.,* **128,** 1899–1927.

Dommenget, D., and M. Latif, 2000: Interannual to decadal variability in the tropical Atlantic. *J. Climate,* **13,** 777–792.

Douville, H., and F. Chauvin, 2000: Relevance of soil moisture for seasonal climate predictions: A preliminary study. *Climate Dyn.,* **16,** 719–736.

Drobinski, P., S. Bastin, S. Janicot, O. Bock, A. Dabas, P. Delville, O. Reitebuch, and B. Sultan, 2009: On the late northward propagation of the West African monsoon in summer 2006 in the region of Niger/Mali. *J. Geophys. Res.,* **114,** D09108, doi:10.1029/2008JD011159.

Duvel, J. P., 1990: Convection over tropical Africa and the Atlantic Ocean during northern summer. Part II: Modulation by easterly waves. *Mon. Wea. Rev.,* **118,** 1855–1868.

Eltahir, E. A. B., 1998: A soil moisture–rainfall feedback mechanism. 1. Theory and observations. *Water Resour. Res.,* **34,** 765–776.

Fink, A. H., and P. M. Reiner, 2003: Spatiotemporal variability of the relation between African easterly waves and West African squall lines in 1998 and 1999. *J. Geophys. Res.,* **108,** 4332, doi:10.1029/2002JD002816.

Fontaine, B., and S. Bigot, 1993: West African rainfall deficits and sea-surface temperatures. *Int. J. Climatol.,* **13,** 271–285.

——, and S. Janicot, 1996: Sea surface temperature fields associated with West African rainfall anomaly types. *J. Climate,* **9,** 2935–2940.

——, S. Louvet, and P. Roucou, 2008: Definition and predictability of an OLR-based West african monsoon onset. *Int. J. Climatol.,* **28,** 1787–1798, doi:10.1002/joc.1674.

Frankignoul, C., and E. Kestenare, 2005: Air–sea interactions in the tropical Atlantic: A view based on lagged rotated maximum covariance analysis. *J. Climate,* **18,** 3874–3890.

Giannini, A., R. Saravanan, and P. Chang, 2003: Oceanic forcing of Sahel rainfall on interannual to interdecadal time scales. *Science,* **302,** 1027–1030.

Grabowski, W. W., J.-I. Yano, and M. W. Moncrieff, 2000: Cloud resolving modeling of tropical circulations driven by large-scale SST gradients. *J. Atmos. Sci.,* **57,** 2022–2040.

Graham, N. E., and T. P. Barnett, 1987: Sea surface temperature, surface wind divergence, and convection over the tropical oceans. *Science,* **238,** 657–659.

Grist, J. P., 2002: Easterly waves over Africa. Part I: The seasonal cycle and contrasts between wet and dry years. *Mon. Wea. Rev.,* **130,** 197–211.

Hagos, S., and K. Cook, 2007: Dynamics of the West African monsoon jump. *J. Climate,* **20,** 5264–5284.

Hamatan, M., G. Mahe, E. Servat, J. E. Paturel, and A. Amani, 2004: Synthèse et évaluation des prévisions saisonnières en Afrique de l'Ouest. *Secheresse,* **15,** 279–286.

Hannay, C., D. L. Williamson, J. J. Hack, J. T. Kiehl, J. Olson, S. A. Klein, C. Bretherton, and M. Kohler, 2009: Evaluation of forecasted southeast Pacific stratocumulus in the NCAR, GFDL, and ECMWF models. *J. Climate,* **22,** 2871–2889.

Held, I. M., T. L. Delworth, J. Lu, K. L. Findell, and T. R. Knutson, 2005: Simulation of Sahel drought in the 20th and 21st centuries. *Proc. Natl. Acad. Sci. USA,* **102,** 17 891–17 896.

Herman, A., V. B. Kumar, P. A. Arkin, and J. V. Kousky, 1997: Objectively determined 10-day African rainfall estimates created for famine early warning systems. *Int. J. Remote Sens.,* **18,** 2147–2159.

Hoffman, R. N., and S. M. Leidner, 2005: An introduction to the near-real-time QuikSCAT data. *Wea. Forecasting,* **20,** 476–493.

Hopson, T., 2006: Operational short-term flood forecasting for Bangladesh: Application of ECMWF ensemble precipitation forecasts. *Geophysical Research Abstracts,* Vol. 8, Abstract 9912.

Huang, B., P. S. Schopf, and J. Shukla, 2004: Intrinsic ocean–atmosphere variability of the tropical Atlantic Ocean. *J. Climate,* **17,** 2058–2077.

Huffman, G. J., R. Adler, B. Rudolph, U. Schneider, and P. Keehn, 1995: Global precipitation estimates based on a technique for combining satellite-based estimates, rain gauge analysis, and NWP model precipitation information. *J. Climate,* **8,** 1284–1295.

Ines, A., and J. Hansen, 2006: Bias correction of daily GCM rainfall for crop simulation studies. *Agric. For. Meteor.,* **138,** 44–53.

Janicot, S., and B. Sultan, 2001: Intra-seasonal modulation of convection in the West African monsoon. *Geophys. Res. Lett.,* **28,** 523–526.

——, and ——, 2007: The large-scale context on the West African monsoon in 2006. *CLIVAR Exchanges,* No. 41 (Vol. 12, No. 2), International CLIVAR Project Office, Southampton, United Kingdom, 11–17.

——, and Coauthors, 2008: Large-scale overview of the summer monsoon over West Africa during the AMMA field experiment in 2006. *Ann. Geophys.,* **26,** 2569–2595.

Kamga, A. F., S. Fongang, and A. Viltard, 2000: Systematic errors of the ECMWF operational model over tropical Africa. *Mon. Wea. Rev.,* **128,** 1949–1959.

Kang, I. S., J. Y. Lee, and C. K. Park, 2004: Potential predictability of summer mean precipitation in a dynamical seasonal prediction system with systematic error correction. *J. Climate,* **17,** 834–844.

Köhler, M., 2005: Improved prediction of boundary layer clouds. *ECMWF Newsletter,* No. 104, ECMWF, Reading, United Kingdom, 18–22.

Lavaysse, C., A. Diedhiou, H. Laurent, and T. Lebel, 2006: African easterly waves and convective activity in wet and dry sequences of the West African monsoon. *Climate Dyn.,* **27,** 319–332.

Maloney, E. D., J. Shaman, and O. Corvallis, 2008: Intraseasonal variability of the West African monsoon and Atlantic ITCZ. *J. Climate,* **21,** 2898–2918.

Marin, F., G. Caniaux, B. Bourlès, H. Giordani, Y. Gouriou, and E. Key, 2009: Why were sea surface temperatures so different in the eastern equatorial Atlantic in June 2005 and 2006? *J. Phys. Oceanogr.,* **39,** 1416–1431.

Matthews, A., 2004: Intraseasonal variability over tropical Africa during northern summer. *J. Climate,* **17,** 2427–2440.

Mekonnen, A., C. D. Thorncroft, and A. R. Aiyyer, 2006: Analysis of convection and its association with African easterly waves. *J. Climate,* **19,** 5405–5421.

Miller, M. J., A. C. M. Beljaars, and T. N. Palmer, 1992: The sensitivity of the ECMWF model to the parameterization of evaporation from the tropical oceans. *J. Climate,* **5,** 418–434.

Mitchell, T. D., and P. D. Jones, 2005: An improved method of constructing a database of monthly climate observations and associated high-resolution grids. *Int. J. Climatol.,* **25,** 693–712.

Mitchell, T. P., and J. M. Wallace, 1992: The annual cycle in equatorial convection and sea surface temperature. *J. Climate,* **5,** 1140–1156.

Mlawer, E. J., and S. Clough, 1997: Shortwave and longwave enhancements in the Rapid Radiative Transfer Model. *Proc. Seventh Atmospheric Radiation Measurement (ARM) Science Team Meeting,* U.S. Department of Energy, San Antonio, TX. [Available online at https://www.arm.gov/publications/proceedings/conf07/extended_abs/mlawer_ej.pdf.]

Molteni, F., T. S. L. Ferranti, F. Vitart, P. Doblas-Reyes, and M. A. Balmaseda, 2007: Predictions of temperature and rainfall anomalies with the ECMWF Seasonal Forecast System-3. *Proc. ECMWF Workshop on Ensemble Prediction,* Reading, United Kingdom, ECMWF, 117–132. [Available online at http://www.ecmwf.int/publications.]

Morcrette, J., 1989: Comparison of satellite-derived and model-generated diurnal cycles of cloudiness and brightness temperatures. *Adv. Space Res.,* **9,** 175–179.

Mounier, F., S. Janicot, and G. N. Kiladis, 2008: The West African monsoon dynamics. Part III: The quasi-biweekly zonal dipole. *J. Climate,* **21,** 1911–1928.

Murphy, A. H., and E. S. Epstein, 1989: Skill scores and correlation coefficients in model verification. *Mon. Wea. Rev.,* **117,** 572–582.

Nicholson, S. E., and J. C. Selato, 2000: The influence of La Niña on African rainfall. *Int. J. Climatol.,* **20,** 1761–1776.

Okumura, Y., and S. P. Xie, 2004: Interaction of the Atlantic equatorial cold tongue and the African monsoon. *J. Climate,* **17,** 3589–3602.

Opokuankomah, Y., and I. Cordery, 1994: Atlantic sea surface temperatures and rainfall variability in Ghana. *J. Climate,* **7,** 551–558.

Paeth, H., and P. Friederichs, 2004: Seasonality and time scales in the relationship between global SST and African rainfall. *Climate Dyn.,* **23,** 815–837.

Palmer, T. N., 1986: Influence of the Atlantic, Pacific and Indian Oceans on Sahel rainfall. *Nature,* **322,** 251–253.

——, and Coauthors, 2004: Development of a European Multimodel Ensemble System for Seasonal-to-Interannual Prediction (DEMETER). *Bull. Amer. Meteor. Soc.,* **85,** 853–872.

Parker, D. J., 2002: The response of CAPE and CIN to tropospheric thermal variations. *Quart. J. Roy. Meteor. Soc.,* **128,** 119–130.

——, and Coauthors, 2005: The diurnal cycle of the West African monsoon circulation. *Quart. J. Roy. Meteor. Soc.,* **131,** 2839–2860.

Piani, C., J. Haerter, and E. Coppola, 2009: Statistical bias correction for daily precipitation in regional climate models over Europe. *Theor. Appl. Climatol.,* **99,** 187–192, doi:10.1007/s00704-009-0134-9.

Pincus, R., H. W. Barker, and J. J. Morcrette, 2003: A fast, flexible, approximate technique for computing radiative transfer in inhomogeneous cloud fields. *J. Geophys. Res.,* **108,** 4376, doi:10.1029/2002JD003322.

Ramel, R., H. Gallée, and C. Messager, 2006: On the northward shift of the West African monsoon. *Climate Dyn.,* **26,** 429–440.

Reed, R. J., A. Hollingsworth, W. A. Heckley, and F. Delsol, 1988: An evaluation of the performance of the ECMWF operational system in analyzing and forecasting easterly wave disturbances over Africa and the tropical Atlantic. *Mon. Wea. Rev.,* **116,** 824–865.

Reynolds, R. W., N. A. Rayner, T. M. Smith, D. C. Stokes, and W. Wang, 2002: An improved in situ and satellite SST analysis. *J. Climate,* **15,** 1609–1625.

Richter, I., and S. P. Xie, 2008: On the origin of equatorial Atlantic biases in coupled general circulation models. *Climate Dyn.,* **31,** 587–598.

Roca, R., J. P. Lafore, C. Piriou, and J. L. Redelsperger, 2005: Extratropical dry-air intrusions into the West African monsoon midtroposphere: An important factor for the convective activity over the Sahel. *J. Atmos. Sci.,* **62,** 390–407.

Rodwell, M. J., and T. N. Palmer, 2007: Using numerical weather prediction to assess climate models. *Quart. J. Roy. Meteor. Soc.,* **133,** 129–146.

Ropelewski, C. F., and M. S. Halpert, 1987: Global and regional scale precipitation patterns associated with El Niño/Southern Oscillation. *Mon. Wea. Rev.,* **115,** 1606–1626.

Rossow, W. B., and R. A. Schiffer, 1991: ISCCP cloud data products. *Bull. Amer. Meteor. Soc.,* **72,** 2–20.

——, A. W. Walker, and L. C. Garder, 1993: Comparison of ISCCP and other cloud amounts. *J. Climate,* **6,** 2394–2418.

Rowell, D. P., C. K. Folland, K. Maskell, J. A. Owen, and M. N. Ward, 1992: Modeling the influence of global sea-surface temperatures on the variability and predictability of seasonal Sahel rainfall. *Geophys. Res. Lett.,* **122,** 905–908.

Servain, J., A. J. Busalacchi, M. J. McPhaden, A. D. Moura, G. Reverdin, M. Vianna, and S. E. Zebiak, 1998: A Pilot Research Moored Array in the Tropical Atlantic (PIRATA). *Bull. Amer. Meteor. Soc.,* **79,** 2019–2031.

Stockdale, T. N., M. A. Balmaseda, and A. Vidard, 2006: Tropical Atlantic SST prediction with coupled ocean–atmosphere GCMs. *J. Climate,* **19,** 6047–6061.

Sultan, B., and S. Janicot, 2003: The West African monsoon dynamics. Part II: The ''preonset'' and ''onset'' of the summer monsoon *J. Climate,* **16,** 3407–3427.

——, ——, and A. Diedhiou, 2003: The West African monsoon dynamics. Part I: Documentation of intraseasonal variability. *J. Climate,* **16,** 3389–3406.

——, ——, and P. Drobinski, 2007: Characterization of the diurnal cycle of the West African monsoon around the monsoon onset. *J. Climate,* **20,** 4014–4032.

Taylor, C. M., F. Said, and T. Lebel, 1997: Interactions between the land surface and mesoscale rainfall variability during HAPEX-Sahel. *Mon. Wea. Rev.,* **125,** 2211–2227.

Thomson, M. C., F. J. Doblas-Reyes, S. J. Mason, R. Hagedorn, S. J. Connor, T. Phindela, A. P. Morse, and T. N. Palmer, 2006: Malaria early warnings based on seasonal climate forecasts from multi-model ensembles. *Nature,* **439,** 576–579.

Thorncroft, C. D., and Coauthors, 2003: The JET2000 project: Aircraft observations of the African easterly jet and African easterly waves. *Bull. Amer. Meteor. Soc.,* **84,** 337–351.

Tiedtke, M., 1993: Representation of clouds in large-scale models. *Mon. Wea. Rev.,* **121,** 3040–3061.

Tompkins, A. M., 2001: On the relationship between tropical convection and sea surface temperature. *J. Climate,* **14,** 633–637.

——, C. Cardinali, J.-J. Morcrette, and M. Rodwell, 2005a: Influence of aerosol climatology on forecasts of the African easterly jet. *Geophys. Res. Lett.,* **32,** L10801, doi:10.1029/2004GL022189.

——, A. Diongue, D. J. Parker, and C. D. Thorncroft, 2005b: African easterly jet in the ECMWF Integrated Forecast System: 4D-Var analysis. *Quart. J. Roy. Meteor. Soc.,* **131,** 2861–2886.

——, K. Gierens, and G. Rädel, 2007: Ice supersaturation in the ECMWF Integrated Forecast System. *Quart. J. Roy. Meteor. Soc.,* **133,** 53–63.

Torrence, C., and G. P. Compo, 1998: A practical guide to wavelet analysis. *Bull. Amer. Meteor. Soc.,* **79,** 61–78.

Verstraete, J. M., 1992: The seasonal upwellings in the Gulf of Guinea. *Prog. Oceanogr.,* **29,** 1–60.

Vialard, J., F. Vitart, M. A. Balmaseda, T. N. Stockdale, and D. L. T. Anderson, 2005: An ensemble generation method for seasonal forecasting with an ocean–atmosphere coupled model. *Mon. Wea. Rev.,* **133,** 441–453.

Vidard, A., D. L. T. Anderson, and M. Balmaseda, 2007: Impact of ocean observation systems on ocean analysis and seasonal forecasts. *Mon. Wea. Rev.,* **135,** 409–429.

Vitart, F., and Coauthors, 2008: The new VarEPS-monthly forecasting system: A first step towards seamless prediction. *Quart. J. Roy. Meteor. Soc.,* **134,** 1789–1799.

Vizy, E. K., and K. H. Cook, 2001: Mechanisms by which Gulf of Guinea and eastern North Atlantic sea surface temperature anomalies can influence African rainfall. *J. Climate,* **14,** 795–821.

Wang, B., and Coauthors, 2008: Advance and prospectus of seasonal prediction: Assessment of the APCC/CliPAS 14-model ensemble retrospective seasonal prediction (1980–2004). *Climate Dyn.,* **33,** 93–117, doi:10.1007/s00382-008-0460-0.

Wentz, F. J., 1997: A well-calibrated ocean algorithm for SSM/I. *J. Geophys. Res.,* **102,** 8703–8718.

Wielicki, B. A., R. D. Cess, M. D. King, A. D. Randall, and E. F. Harrison, 1995: Mission to Planet Earth: Role of clouds and radiation in climate. *Bull. Amer. Meteor. Soc.,* **76,** 2125–2153.

——, B. R. Barkstrom, E. F. Harrison, R. B. Lee, G. L. Smith, and J. E. Cooper, 1996: Clouds and the Earth's Radiant Energy System (CERES): An Earth Observing Eystem experiment. *Bull. Amer. Meteor. Soc.,* **77,** 853–868.

Wolff, J. O., E. Maier-Reimer, and S. Legutke, 1997: The Hamburg Ocean Primitive Equation Model. DKRZ Tech. Rep. 13, Hamburg, Germany, 98 pp.

Yu, L., X. Jin, and R. A. Weller, 2006: Role of net surface heat flux in seasonal variations of sea surface temperature in the tropical Atlantic Ocean. *J. Climate,* **19,** 6153–6169.

Zhang, C. D., 1993: Large-scale variability of atmospheric deep convection in relation to sea surface temperature in the tropics. *J. Climate,* **6,** 1898–1913.

Zheng, X., E. A. B. Eltahir, and K. A. Emmanuel, 1999: A mechanism relating tropical Atlantic spring sea surface temperature and West African rainfall. *Quart. J. Roy. Meteor. Soc.,* **125,** 1129–1164.